ACS Catalysis

Review

pubs.acs.org/acscatalysis

Catalyst Design with Atomic Layer Deposition

Brandon J. O'Neill,[†,¶] David H. K. Jackson,[†,‡] Jechan Lee,[†] Christian Canlas,[§] Peter C. Stair,[∥,⊥] Christopher L. Marshall,[∥] Jeffrey W. Elam,[§] Thomas F. Kuech,[†,‡] James A. Dumesic,[†] and George W. Huber*[,†]

[†]Department of Chemical and Biological Engineering, [‡]Materials Science Program, University of Wisconsin−Madison, Madison, Wisconsin 53706, United States

[§]Energy Systems Division, [∥]Chemical Science and Engineering, Argonne National Laboratory, Argonne, Illinois 60439, United States

[⊥]Department of Chemistry, Northwestern University, Evanston, Illinois 60208, United States

ABSTRACT: Atomic layer deposition (ALD) has emerged as an interesting tool for the atomically precise design and synthesis of catalytic materials. Herein, we discuss examples in which the atomic precision has been used to elucidate reaction mechanisms and catalyst structure−property relationships by creating materials with a controlled distribution of size, composition, and active site. We highlight ways ALD has been utilized to design catalysts with improved activity, selectivity, and stability under a variety of conditions (e.g., high temperature, gas and liquid phase, and corrosive environments). In addition, due to the flexibility and control of structure and composition, ALD can create myriad catalytic structures (e.g., high surface area oxides, metal nanoparticles, bimetallic nanoparticles, bifunctional catalysts, controlled microenvironments, etc.) that consequently possess applicability for a wide range of chemical reactions (e.g., CO_2 conversion, electrocatalysis, photocatalytic and thermal water splitting, methane conversion, ethane and propane dehydrogenation, and biomass conversion). Finally, the outlook for ALD-derived catalytic materials is discussed, with emphasis on the pending challenges as well as areas of significant potential for building scientific insight and achieving practical impacts.

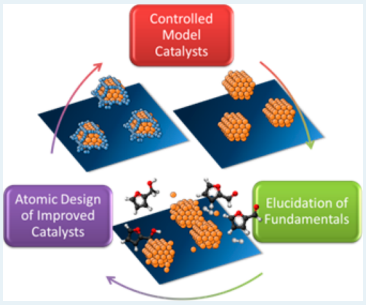

KEYWORDS: *atomic layer deposition, ALD, catalyst overcoating, metal nanoparticles, bimetallic nanoparticles, controlled synthesis, catalyst design, mechanism elucidation*

1. INTRODUCTION

1.1. The Motivation for Atomically Designed Catalysts. Catalysis is an essential technology for accelerating and directing chemical transformations.[1] It is a key to realizing environmentally benign, economical processes for the conversion of fossil-based feeds. Catalysis is also key to developing new technologies for creating value from alternative feedstocks, such as biomass, carbon dioxide, and water. Catalysts, whether chemical, biological, or a combination of the two,[2] are the primary means for industrially converting carbonaceous feeds (oil, gas, coal, and biomass) to useful products such as fuels and chemicals. Globally, the catalyst market is estimated to be ∼$15 billion per year, resulting in a net positive balance of trade in the U.S. and an estimated global economic impact of ∼$15 trillion per year: a 1000-fold multiplier of economic impact.[3] In fact, approximately one-third of the U.S. GDP can be tied directly to catalytic technologies,[3] and nearly 95% of fuels and chemicals have come through one or more catalytic steps. Nearly every major industry is directly enabled by catalytic technology, be it energy, chemicals, pharmaceuticals, healthcare, food processing, agriculture, consumer products, or environmental remediation.

For most industrial processes, the preferred catalysts are heterogeneous (normally a solid catalyst reacting with a gas or liquid substrate) because these solid catalysts can be easily separated from the final product. Current approaches for synthesizing heterogeneous catalysts, including impregnation, ion exchange, and precipitation, have been used for over a century. While these techniques represent the "state-of-the-art," they result in inhomogeneous particle sizes and compositions. In the case of supported metal catalysts, the resulting mixture of metal sites can produce a mixture of reaction products rather than the single, preferred site. This nonuniformity of sites creates a struggle to find balance between activity, selectivity, and stability. Great strides were made throughout the 20th century in improving activities for many catalytic processes by several orders of magnitude. The challenge in the 21st century is to improve the selectivity of the catalysts to convert specific feedstocks into specific products with little or no waste associated with undesirable side reactions. This search for atom-efficient chemical transformation has been particularly important over the past decade as researchers have searched for ways to more efficiently utilize alternative and oftentimes more expensive feedstocks (e.g., biomass conversion to fuels and chemicals) as sustainable and environmentally benign replacements for fossil-based feeds.

Many processes for the conversion of biologically derived feedstocks to marketable products (e.g., cellulose to sugars,

Received: November 24, 2014
Revised: February 3, 2015
Published: February 6, 2015

DOI: 10.1021/cs501862h
ACS Catal. 2015, 5, 1804−1825

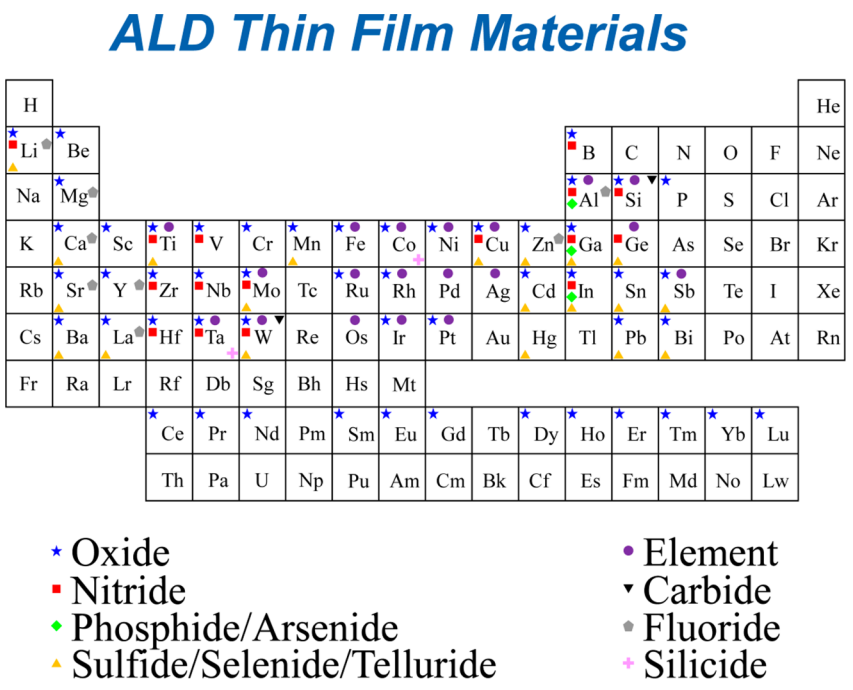

Figure 1. Overview of elements used for ALD materials. Figure adapted from reference.[21]

sugars to ethanol, etc.) have relied on enzymatic catalysis. Indeed, enzymes have many advantages in that they can be highly active and selective, processing only a single feedstock and forming only one specific product. While being selective, enzymes require constant replacement and lack the flexibility to operate under a variety of conditions. For example, many enzymatic systems are designed to work at body temperature (37 °C) and neutral pH, and they tend to denature outside of these conditions. We can hope to harness some of the benefits nature evolved into enzymes by learning how to tailor specific sites and localized reaction environments to target specific chemical transformations. The design of catalysts in this manner is common in molecular catalysis, and although molecular catalysts have advantages over biologically derived catalysts, they still lack the robustness provided by inorganic materials in many catalytic applications. The challenge, therefore, is to create inorganic (or hybrid) analogues to enzymatic systems that maintain high activity and selectivity but with enhanced stability under a broad range of harsh temperatures, pressures, and solvents.

The challenge of simultaneously improving catalytic activity, selectivity, and stability is shared by biological and inorganic catalysts alike. One common way of improving catalytic activity for heterogeneous, inorganic catalysts is modifying the current "state-of-the-art" synthesis procedures to maximize the reactive surface area of the material. In the case of supported catalysts, these techniques normally result in nanoparticles with a distribution of sizes and chemical environments (i.e., not a single active site) and, in turn, chemical selectivity. This dispersity in possible active sites also poses a challenge in developing fundamental knowledge regarding mechanisms of surface reactions on heterogeneous materials. The understanding and optimization of the catalytic materials is convoluted with the reaction mechanism itself, and realistically, the two cannot be considered independently. In addition, the resulting dispersed nanoparticles are often unstable, which is especially important in harsh liquid-phase conditions that will be required for most biological and biomass upgrading processes.[2] Therefore, an important goal is to control the size, shape, and morphology of supported nanoparticles to improve selectivity. Importantly, these challenges have consequences that are simultaneously practical and academic, and advancement requires realistic solutions to practical problems based on rigorous scientific understanding.

To achieve the goals outlined above requires a method for controlling the synthesis of catalytic materials on the atomic scale. One such method, atomic layer deposition (ALD), has been shown to be effective at controlling metal and metal oxide sites and improving catalytic activity, selectivity, and longevity. Whereas other methods of controlled synthesis (that fall outside the scope of this perspective) have been studied in the past, many have been limited to a narrow set of materials and conditions. ALD, on the other hand, has the advantage of being able to apply self-limiting films or nanoparticles (depending on conditions) of nearly any material (Figure 1). Some advantages of the self-limiting nature of ALD include uniform surfaces, high conformity to surface features, control and accuracy of atomic level thickness, and extraordinary reproducibility. Accordingly, ALD provides a controlled method in which atomically precise growth is produced, precisely what is needed to address the catalytic challenges just outlined.

In the past few years, the use of ALD for self-limiting synthesis of catalysts within nanostructured environments has been demonstrated. Important examples include combining theoretical insights with experimental studies to provide a more detailed understanding of relevant ALD precursor surface reaction chemistry[4] and using ALD to control metal growth on surfaces,[5] alloy and core−shell catalysts,[6−9] and protective and functional overcoatings.[10−15] These new catalysts show improved selectivity for specific catalytic reactions and are more stable, even in the high temperature, aqueous conditions of biomass conversion.[11] Even base-metal nanoparticle catalysts have been synthesized in which edge and defect sites were selectively poisoned by ALD-derived overcoats, leading to

DOI: 10.1021/cs501862h
ACS Catal. 2015, 5, 1804−1825

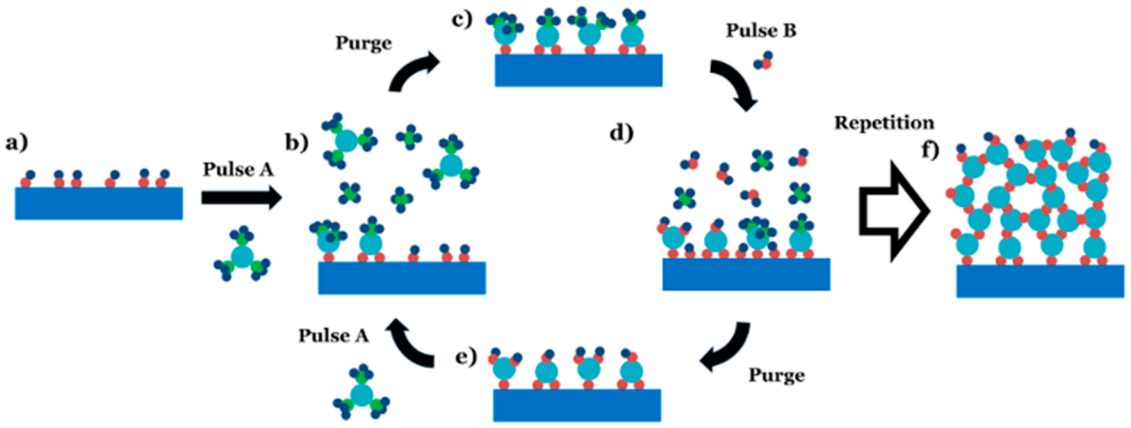

Figure 2. Schematic representation of film ALD using a binary (AB) precursor system. The schematic shows (a) substrate with reactive sites, (b) pulsing of the first precursor and formation of active sites reaction byproducts, (c) purging of byproducts and unreacted precursor, (d) pulsing of the second precursor, (e) purging of byproducts and second precursor that is unreacted, and (f) film resulting from several ALD cycles.

lower-cost catalysts with improved stability and selectivity.[11−13,16,17] In addition, highly active and selective bimetallic catalysts in which the location of each metal is precisely controlled could be prepared by ALD.[7−9] Furthermore, combining state-of-the-art in situ and ex situ spectroscopic techniques (XANES, EXAFS, TEM, STM, SAXS, etc.) with the atomically precise synthesis of ALD provided in-depth structural and electronic characterization of the catalytic materials, elucidating the scientific basis on which future applications can be developed.

1.2. A Brief ALD History. Atomic layer deposition, defined as synthesis using alternating, saturating gas−solid reactions, was coinvented by two groups working independently.[18] The first group, from which modern ALD is most directly derived, led by Tuomo Suntola in Finland, invented "atomic layer epitaxy" (ALE) as a strategy to fabricate electroluminescent displays. The first ALE patent was applied for in November, 1974, and it described a method for depositing ZnS films using alternating exposures to elemental Zn and S.[19] Later work by Suntola's group discovered that molecular precursors, namely $ZnCl_2$ and H_2S, yielded a more production-worthy process since it could be performed under viscous flow conditions rather than requiring a high vacuum environment. These early efforts were directed toward electronic applications and focused primarily on micrometer-thickness films requiring many thousands of ALD cycles. An example of this early achievement was the fabrication and installation of a flight-information display board at the Helsinki−Vantaa airport in 1983 that operated for 15 years using ALD Mn-doped ZnS as the electroluminescent material and ALD Al_2O_3−TiO_2 nanolaminate as the dielectric.

In the second historical group, Professors Aleskovskii and Koltsov of the USSR Academy of Sciences developed "molecular layering" (ML) as a means to deposit metal oxides using alternating exposures to metal chloride precursors and water. Conference proceedings from the early 1960s describe TiO_2 and GeO_2 ML, but these studies were overlooked by researchers from outside the Soviet Union because they were published only in Russian.[18] Nevertheless, these early studies gave birth to ALD for catalyst synthesis, since they focused on the early stages of thin film growth from 1 to 10 cycles and utilized high surface area substrates such as silica gel. Indeed, a Russian patent from 1972 describes Cr(III) oxide ML on silica gel for use as a dehydrogenation catalyst.[20]

Later, in Japan, ALD processes were referred to as molecular layer epitaxy. The term epitaxy refers to the growth in which the deposited film has a crystallographic relationship to the crystal structure of the underlying substrate. ALD coatings are frequently amorphous in nature, so "deposition", rather than "epitaxy", more appropriately describes all processes falling under this category, and consequently, this is reflected in the modern nomenclature, although limited anachronistic examples of the older nomenclatures can still be found. In addition, molecular layer deposition (MLD) has been developed as an analog to ALD using exclusively organic compounds to deposit thin film polymer layers.

Most of the early pioneering work in ALD catalyst synthesis was performed at Microchemistry Ltd. by Haukka and Suntola in the 1990s. This work demonstrated the capability to coat multikilogram quantities of high-surface-area supports with catalytically active metal oxides and extended the range of ALD precursors to include organometallics such as beta-diketonates, alkyls, and alkoxides. More importantly, the Microchemistry group showed that the saturation surface coverage of metal-oxo species could be controlled by adjusting the steric bulkiness of the precursor ligands or by preheating the substrate to partially dehydroxylate the surface. They also revealed that blocking agents could be employed to influence the distribution of ALD surface species and that differences in surface reactivity (e.g., toward Si−OH groups or Si−O−Si bridging groups) could also be exploited to control surface speciation. Mixed-metal oxide catalysts were also synthesized by executing multiple ALD cycles using different precursor chemistries, providing early inspiration for later works to utilize ALD as a means of atomically tailoring physical and chemical properties. Later studies performed at the Helsinki University of Technology extended ALD catalyst synthesis to include noble metals. Importantly, these early studies laid the ground for much of the nanostructured ALD catalyst research that followed.

A surge in ALD research and development began in the late 1990s and early 2000s and continues to the present day, driven by the needs of the microelectronics industry. For instance, the requirement for "high-k" materials to replace SiO_2 as the gate dielectric in transistors motivated research into the oxides of Hf, Zr, Ta, and other materials. As a consequence, the palate of available ALD materials has greatly expanded to include much of the periodic table and includes oxides, nitrides, sulfides, and metals (Figure 1).[21] For any given material, multiple ALD

DOI: 10.1021/cs501862h
ACS Catal. 2015, 5, 1804−1825

chemistries have been developed so that today the number of available ALD processes numbers over 1000. This situation is ideal for catalyst synthesis because it permits a vast selection of catalyst, support, and promoter materials to precisely tune the catalytic behavior. The surge in ALD activity for microelectronics caught the attention of researchers in other fields who sought to adopt the ALD microelectronic approach of depositing controlled functional layers for nanomaterials synthesis in applications such as photovoltaics, energy storage, and sensing. ALD layers can be used to functionalize nanoporous supports such as carbon nanotubes (CNTs)[22,23] and anodic alumina[24,25] to impart desirable chemical, physical, and electronic properties to the supports. The support can be retained in the final device or used merely as a template to be later etched or dissolved. Experimental, analytic, and numerical studies of infiltration and coating have been performed to better understand the processes underlying ALD nanomaterials growth, and these studies are invaluable to ongoing research in ALD for catalyst synthesis.

Note that our review of the ALD catalyst literature reflects the fact that the focus of the majority of the work has been on the development and synthesis of ALD materials rather than on a detailed exploration of their catalytic properties. For the continued development of ALD catalysts, additional careful investigations of the performance of ALD catalysts and direct comparisons with how they differ in structure and performance from catalysts synthesized by more traditional means will be necessary.

2. ATOMIC LAYER DEPOSITION PROCESS AND EQUIPMENT

2.1. Atomic Layer Deposition Processes for Catalysts.

ALD is a vapor-phase deposition technique relying on discrete pulsing of chemical precursors that act as sources for component elements of the desired film (Figure 2). One precursor is typically a high vapor pressure metal precursor, such as trimethylaluminum (TMA),[26] hafnium tetrachloride,[27] or titanium isopropoxide.[28] The reaction of this metal precursor with the substrate is referred to as the first half-reaction (Figure 2a,b), in which the reactive ligands of the metal precursor are partially removed by reaction with active sites on the substrate surface. When the first half reaction reaches completion, the precursor pulse is stopped, and excess unreacted precursor and reaction byproducts are purged with an inert gas or evacuated at high vacuum (Figure 2b,c). The second half reaction usually contributes an oxygen component when depositing oxides or a reducing agent in the case of metals (although many other examples including nitrides, sulfides, etc. exist; see Figure 1) and removes the remaining ligands of the metal precursor, regenerating the active sites and completing the reaction cycle (Figure 2d). The reactor is purged or evacuated again following completion of the surface reaction (Figure 2e), and the cycle can be repeated until the desired thickness is achieved (Figure 2f). The self-limiting nature of the half-reactions imparts excellent film conformality and thickness control to this process, and variations of this basic process can lead to the synthesis of more complex structures. Deposition by ligand exchange reactions (Figure 2) is the most common ALD mechanism; however, self-limiting growth can also be achieved by other mechanisms, such as combustion or reduction in the case of noble metals[29] and sacrificial exchange reactions in the case of W and Mo ALD.[30]

It is important to distinguish ALD from chemical vapor deposition (CVD), a related vapor-phase deposition process, which employs a continuous precursor stream and is characterized by nonself-limiting growth. While broadly used, CVD can lack the degree of conformality and digital thickness control that make ALD so critical for applications in catalysis. CVD has been used extensively to produce catalysts since the 1970s;[31] however, the precision of the ALD process and the increase in availability of suitable chemical reaction schemes and ALD-specific reactors has led to a recent growth in the use of ALD in catalyst synthesis. It should be noted that CVD-like growth can occur within the ALD process with a loss of the self-limiting growth mode. There is a temperature regime for each specific reaction pathway within which ALD self-limiting growth can be achieved. ALD attempted at either too high or too low a reaction temperature is considered to be outside the so-called "ALD window"[32,33] and, thus, sacrifices the benefits that make ALD an attractive mode of catalyst synthesis. In general, both self-limiting and continuous growth processes are present, but conditions within the ALD window can be chosen such that kinetically slow, continuous growth modes may be considered insignificant.

To achieve ideal conformality with ALD on high-surface-area materials found in typical catalyst supports, long precursor pulse times may be necessary to achieve surface saturation. This increased pulse time is due to limitations of reactant mass transport and precursor partial pressure at short times, and it increases the possibility of non-self-limiting growth. An example of this behavior is found in the coating of trench structures with hafnium oxide, which can result in slight nonuniformity, with coatings at the tops of the trenches being thicker than at the bottoms.[34] The top of the trench is exposed to the Hf sources at a higher partial pressure than seen in the bottom of the trench, leading to a higher reactant dose at the opening and an increased rate of continuous or CVD-like deposition in addition to the purely self-limited growth rate. Reports on other materials systems have noted the observation of a deviation from purely self-limited growth, such as in the deposition of Al_2O_3 on battery $LiCoO_2$ cathode powders,[35] the deposition of tungsten oxide on TiO_2 powders,[36] and in a TiN process with precursors decomposing during long pulses.[37] Although the ideal self-limiting growth mode is commonly used to describe ALD, deviations from self-limited deposition can play a significant role in the application of ALD to catalysts. Researchers looking to leverage the advantages of ALD in catalysts need to be cognizant of these modest but important deviations from ideal behavior and realize that ALD and CVD are part of the same growth continuum.

The example of ALD shown in Figure 2 is a binary process driven by the formation of thermodynamically favored surface species as the half-reaction products. The kinetic processes comprising two precursors are typically thermally driven and are referred to as thermal AB ALD processes. Although the AB process is commonly employed, other variations exist. For example, three different precursors can be used, such as aminopropyl triethoxysilane–H_2O–ozone[38] or $Pd(hfac)_2$–TMA–H_2O, in an ABC sequence.[39] The complexity of the reaction sequence can be further increased to create ABCB processes, which have been used in the deposition of mixed oxides, such as TMA–H_2O–Cp_2Mg–H_2O.[13,40] This flexibility in reaction sequences is a significant part of what makes ALD such an attractive method of catalysts synthesis.

DOI: 10.1021/cs501862h
ACS Catal. 2015, 5, 1804–1825

The simultaneous introduction of specific reactants can open possible process windows that extend the previously mentioned ALD window by catalyzing the half-reaction. This coaddition or copulsing of specific reactants, which do not remain in the film yet interact with other ALD reactants, can facilitate the film deposition process. These catalyzed ALD processes, usually referred to as catalytic ALD, may be written as an A/C−B/C sequence. The most well studied example is the use of an amine catalyst to facilitate the reactions between the surface and precursors, with the primary example being to enable low temperature deposition of SiO_2.[41,42] Si precursors such as $SiCl_4$ and TEOS are not sufficiently reactive within the range of desired ALD temperatures (~30 to 250 °C).[41,42] Utilizing amine catalysts enables the deposition of SiO_2 at room temperature, avoiding potential thermally induced damage to other system components, such as those on an existing electronic circuit or supported metal nanoparticles. A proposed catalytic reaction mechanism is shown in Figure 3 where

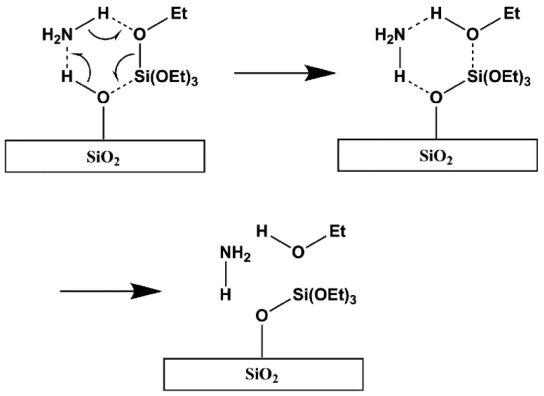

Figure 3. Proposed mechanism for Lewis base catalysis of SiO_2 atomic layer deposition during the $Si(OEt)_4$ half-reaction using NH_3. (a) NH_3 forms a six-membered ring complex with silanol and $Si(OEt)_4$, (b) pushing electrons in the six membered ring complex, creating a more reactive and nucleophilic surface oxygen, (c) resulting in a Si surface species, NH_3, and the reaction byproduct ethanol.

ammonia is hypothesized to form hydrogen bonds with surface silanol groups, thus catalyzing the deposition of $SiCl_4$ by making the hydroxyl oxygen more nucleophilic.[42] An alternative method for rapid SiO_2 ALD involves the limited polymeric growth of Si precursors catalyzed by an ALD deposited Al site.[43]

In contrast to thermally or catalytically driven ALD, growth modes may also be enhanced using the in situ transfer of energy to precursors to generate reactive molecules such as ozone or the metastable species found in plasmas. Energy-enhanced ALD (EE-ALD) is used as an umbrella term to encompass a variety of methods used to transfer energy to precursors before they reach the substrate. EE-ALD methods include plasma-enhanced ALD (PE-ALD),[44] hot wire ALD,[45] and ALD processes using ozone.[34,38,46−49] Ozone can be generated with oxygen plasma or through the use of UV light irradiation. EE-ALD techniques are typically employed to reduce the deposition temperature, to circumvent the need for water as the oxygen precursor, or to increase growth rates.[49] Careful design of processing and reactor conditions, including the wall material, are important considerations in EE-ALD methods, especially PE-ALD, because the walls can greatly affect the lifetime of the reactive species. For example, the radical recombination on reactor walls can be 3 orders of magnitude higher than on a SiO_2 surface.

The least energetic of the EE-ALD techniques is called radical enhanced ALD (REALD), which typically utilizes plasma generated through a RF coupled source, electron-cyclotron-resonance, or surface-wave-type plasmas powdered by a microwave source.[44,49] The source is positioned sufficiently far from the sample that ions generated in the plasma are quenched as a result of recombination before they reach the sample, and remaining radicals act as precursors to film growth. Another technique used to generate radicals as precursors is hot-wire ALD, which uses a filament heated to ~1300−1900 °C placed near the inlet, on which precursors are cracked before entering the reactor.[45,49] Remote plasma ALD is similar to REALD; however, a remote plasma source is positioned sufficiently close to the reactor that the concentration of ions reaching the sample is controlled and does not necessarily diminish to zero.[44,49] The remote plasma source in this case is separate from the reaction chamber, but the substrate can experience a small concentration of impinging ions and a high radical flux. The EE-ALD approach with the highest amount of athermal energy directed to the growth front is direct plasma ALD. This approach involves an electrical connection between one of the plasma electrodes and a substrate, creating a near-surface electric field perpendicular to the surface, directing and accelerating ions to the growth front.[44,49] The kinetic energy of the ions can be transferred to the adsorbed species, leading to an enhanced reaction rate at low substrate temperatures. The required electrical connectivity is often difficult to achieve, and hence, direct plasma use on powders poses significant obstacles. The EE-ALD approaches most relevant to catalysis are therefore ozone ALD, radical enhanced ALD, and remote plasma ALD. The growth of AlN[50] and TiN[51] on powders using NH_3 plasma has been used to demonstrate remote plasma ALD.

A wide range of materials may be deposited and coated by ALD. The self-limiting growth mode allows for conformally coated substrates in almost any geometry,[52−57] and selective coating may be achieved by control over the nature and density of active species on the substrate.[11,58,59] ALD layers can be uniformly developed over high-aspect-ratio, structured surfaces with complex geometries, provided that all of the surface has appropriate reactive sites. The possible materials coated by ALD for catalysis and electrocatalysis range from planar-surface wafers to hierarchically structured mesoporous oxides,[54,55] zeolites,[56,57] high-aspect-ratio nanostructures (ie. nanowires,[60] nanotubes[22,23]), complex self-assembled surfactants,[53] and block copolymers.[61] Furthermore, the choice of the ALD precursors, surface preparation, and deposition conditions allows for the production of pinhole-free coatings, porous coatings,[10,11,62] coatings with compositionally controlled gradients,[13,40,63] nanolaminates,[64] nanoparticles,[65−67] and core−shell structures.[8,68,69] This wide array of synthesis approaches to the ALD process has only begun to be exploited for catalytic applications.

The structure and composition of an ALD film is dependent on the choice of precursor. In addition to oxides, ALD nitrides,[37,70,71] sulfides,[72] carbides[73] and other binary alloys have been deposited by choosing half-reaction schemes. Metals may also be deposited using a reducing agent instead of an oxidant.[8,66,67,74,75] For example, the processes for TiO_2 and Al_2O_3, may be modified so that the H_2O pulses are replaced with NH_3 pulses, resulting in the growth of TiN[71,76] and AlN.[77]

DOI: 10.1021/cs501862h
ACS Catal. 2015, 5, 1804−1825

In the case of some ALD-grown oxides, the choice of oxygen-containing source can change the bonding and oxygen content.[46] The specific reactants, while nominally generating films of the same composition, can affect the detailed structure and defect concentration. For example, AlO_x films grown with ozone have been found to contain a lower concentration of Al−Al bonds and O−H bonds than AlO_x grown with H_2O, effectively giving ALD another degree of control over the resulting atomic structure.[46]

In addition to the deposition of conformal coatings, nanoparticles may also be formed on a surface through an appropriate choice of precursors, substrate, and conditions. Nanoparticle formation is especially notable in the deposition of metals for catalysis, in which ALD provides exceptional control over particle size.[65−67] The initial formation of sparsely spaced metal clusters or islands serve as nucleation points during the ALD process. Nanoparticle growth proceeds through an island growth mode often referred to as a Volmer−Weber growth mechanism.[78] The metal precursors can have a stronger interaction with the preexisting deposited metals than with the substrate, leading to the preferential formation of islands over conformal films. These interactions among metal precursors, substrates, and surface metal deposits in ALD have been demonstrated in certain systems to allow core−shell metal nanoparticles to be produced with a high degree of compositional control.[8,68,69]

The selective adsorption of molecules, blocking or consuming active sites prior to the initiation of the ALD cycles, prevents these sites from participating in ALD film formation, creating templates that result in a selectively coated surface. The templates can be removed after the ALD process, creating a controlled porosity or the formation of microstructure in the ALD film. Selective coating by ALD was first developed through the lithographic patterning of surfaces with unreactive organosilanes.[59] The planar templating approach was extended to powders by grafting unreactive template molecules onto TiO_2 particles.[79] The template molecules serve to block ALD coating, resulting in the formation of "nanobowls" that allowed for finely tuned, shape-selective sieving of reactant molecules by controlling the size and shape of the template as well as the thickness of the film.[79] Another example of the atomic selectivity in the ALD synthesis of catalysts has also been demonstrated in the deposition onto metal surfaces, in which edge and corner sites were significantly more reactive with the coating precursors than the close packed facets.[10,11] If excess ALD cycles were used, the ALD films coalesced, completely encapsulating the metal, but subsequent high temperatures treatment led to the formation of pores in the coating through the densification of the ALD film, again leading to a selective coating on the buried metal.[8] These pores allow the diffusion of reactants through the coating to undergo chemical transformation on the metal surface.

An emerging field within ALD is the production of organic and hybrid inorganic−organic materials. These techniques include the growth of inorganic materials on organic substrates, the growth of polymers, and the growth of hybrid inorganic−organic films. Recent studies using organic substrates have covered the deposition of model inorganic films such as Al_2O_3 onto substrates such as polymers,[80] nanofibers,[81] and surfactants.[53] Techniques that utilize organic molecules exclusively as precursors, or organic molecules in conjunction with metal precursors, are categorized as MLD.[82,83] A class of hybrid inorganic−organic materials produced using this technique are the "metalcones" (i.e., alucone, zincone, and titanicone).[82] The simplest example of a metalcone process is the TMA−ethylene glycol process to produce alucone.[84] The alcohol groups of the ethylene glycol react with the methyl groups of TMA in a fashion similar to the typical TMA−H_2O process, with ethylene glycol spacers linking molecular AlO_x layers. Metalcone films can have excellent compliance[82] and may be pyrolized to produce graphitic alloys[85] or highly porous oxides.[62]

2.2. ALD Reactors for Catalysts. Many ALD processes have been developed primarily for coating planar substrates, such as silicon wafers. New designs and approaches are required to utilize ALD processes on powders on both the research and industrial scales. Powders present the most dramatically different case from the typical planar Si wafer, with increased diffusion times required for precursors to travel through pores on the mesoscale, and orders of magnitude more surface area, which require correspondingly longer reaction times or higher reactant partial pressures in the ALD reactor. Many attempts have been made to agitate particle beds to decrease diffusion times and prevent particle agglomeration. In this article, we briefly describe different ALD reactor configurations. A more detailed article discussing the various techniques to use ALD for coating of powders may be found elsewhere.[86]

The simplest and most established approach to the coating of powders consists of a static bed of particles into which the precursor vapors must diffuse and permeate to reach and coat all surfaces. The bed may be in a crucible or tray supported on a heating stage,[86] or it may be in a flow tube with a specifically designed tray, such as that seen in Figure 4.[87] The diffusion kinetics for this type of reactor configuration may be simplified to a model that treats the bed as a series of channels between particles.[88]

Analytical solutions to this growth model can be obtained to describe the ALD growth process. These solutions were important in developing a fundamental understanding of the ALD processes.[86,92] Assuming realistic channel dimensions and reaction conditions, a powder or particle bed depth of greater than a few hundred micrometers would require precursor residence times that are unreasonably long for practical applications (greater than a few minutes per precursor pulse). Consequently, various approaches to enhance the reactant contact with the particle surface in a static bed have been developed. Precursors may continuously flow through the reactor under an active pressure drop, permitting a high reactant partial pressure to be present throughout the reaction. Alternatively, the precursors may be dosed and held in a static, nonflowing reactor, allowing a "soak time" for thorough reactant diffusion and reaction, leading to greater precursor utilization. This static bed approach is well suited for the laboratory scale; however, batch size is typically limited to several grams.

Particle coating in a fluidized bed is a standard industrial approach to powder processing; however, the use of fluidized bed reactors for ALD is less common.[31] An example of a fluidized bed ALD reactor design is shown in Figure 5a, and a few fluidized bed ALD reactor options are now commercially available with a range of features and functionality. Fluidized bed ALD has several advantages, including (1) the ability to operate between vacuum and ambient pressure (e.g., Pt ALD on TiO_2);[93] (2) demonstrated scalability of the fluid bed design (e.g., fluidized catalytic cracking), providing confidence in the ability to produce larger quantities of catalyst; (3) well-mixed

DOI: 10.1021/cs501862h
ACS Catal. 2015, 5, 1804−1825

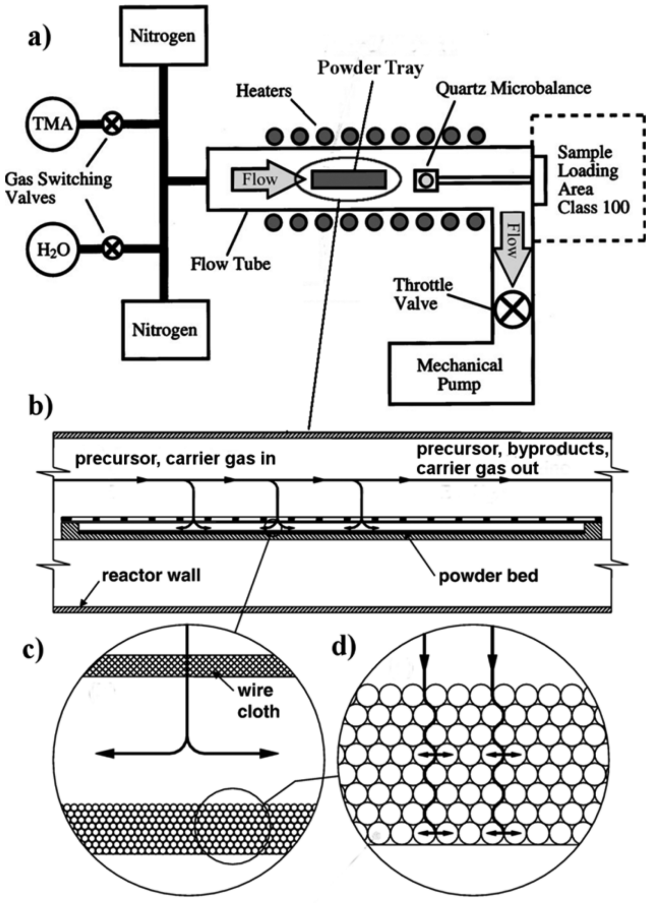

Figure 4. (a) ALD reactor schematic showing precursors, carrier gas, heated flowtube, valves, and pump, with a powder tray in the flowtube. (b) Side view of the powder tray showing precursors entering the reactor and diffusing into the powder bed to coat the powder. (c) Close-up showing precursors diffusing through the wire cloth on the powder bed to prevent loss of the powder. (d) Close up showing precursor diffusion into the powder bed and into the pores of the powder. Part a adapted with permission from Elam et al., Copyright 2002, AIP Publishing LLC.[89] Parts b–d adapted with permission from Libera et al., Copyright 2008, Elsevier B.V.[87]

solid particles; (4) improved gas transport compared with a static bed; and (5) a very large ratio of powder to reactor wall surface area (allowing efficient use of precursor by preventing its loss onto the reactor walls). In addition, because all of the precursor must pass through the fluidized powder bed, precursor usage efficiency can be greatly increased, which has the practical implication of greatly reducing synthesis time and cost. Progress of the reaction can be monitored using in situ mass spectrometry to determine pulse sequencing times, optimize deposition speed, and optimize precursor utilization.[90] Fluidization may also be aided by the addition of baffles, vibration of the bed, or by a rotating propeller.[90] Finally, it is important to note that particles typically have a range of sizes, and this will influence the fluidization behavior.[90,94] In addition, nanoparticles typically fluidize as large highly porous aggregates, but the nanoparticles can shed and recombine from aggregate to aggregate, which allows all of the individual particles to be coated evenly.[95]

The typical ALD process relies on temporal separation of the precursors through the inclusion of a purge stage between precursor pulses, with the substrate remaining fixed in space. An alternate, albeit less well proven, concept is spatial ALD, in which the precursors are dosed continuously in different zones of the reactor while the substrate is moved through space between regions.[98] This design offers the advantage of continuous processing. Studies on spatial ALD have shown promising preliminary results in the scale-up of wafer-coating systems.[98] A conceptual design for a spatial powder ALD system is shown in Figure 6. Figure 6a shows the theory of operation of a semicontinuous spatial ALD reactor based on a valved reservoir concept.[96,97] The powder would be supported above a powder-compliant valve while the precursor vapor is filled into a reservoir below (Figure 6ai). The pressure in the powder reservoir would be lower than in the precursor reservoir so that when the valve is opened, the precursor gases escape upward and the powder would be partially fluidized (Figure 6aii). The precursor would react with the powder, and then the powder falls into the reservoir below (Figure 6aiii). A CAD drawing of this semicontinuous reactor concept is shown in Figure 6b.[97] Another spatial ALD design has been proposed by a group in Delft with promising

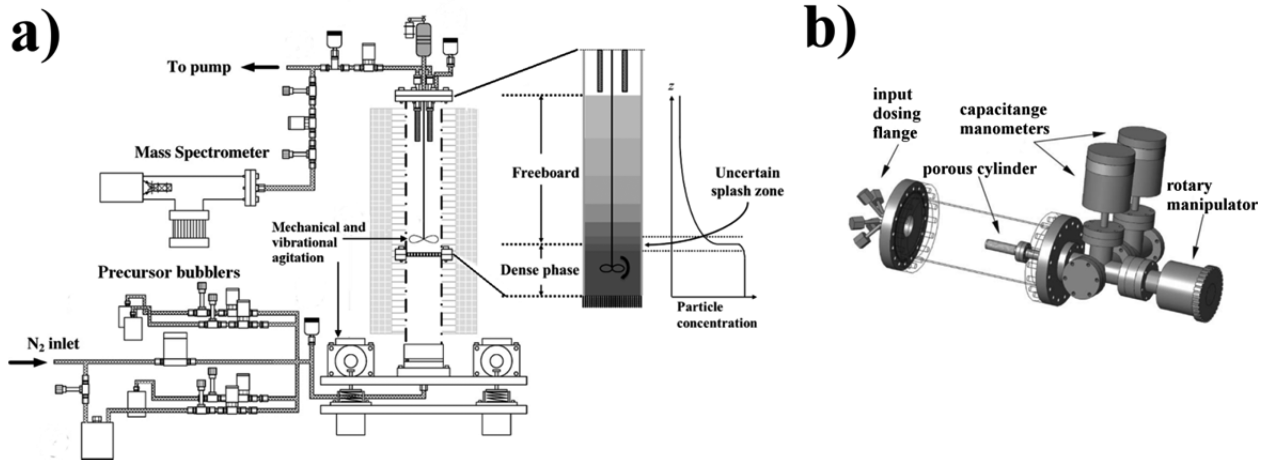

Figure 5. (a) Schematic of a fluidized bed reactor for particle ALD. The reactor has an online in situ mass spectrometer, a stirring agitator, and vibration enhanced fluidization. Close-up on the right shows particle concentration as a function of height in the bed. Adapted with permission from Elsevier B.V., Copyright 2007.[90] (b) Schematic of a rotary bed ALD reactor. Reproduced with permission from AIP Publishing LLC, Copyright 2007.[91]

DOI: 10.1021/cs501862h
ACS Catal. 2015, 5, 1804–1825

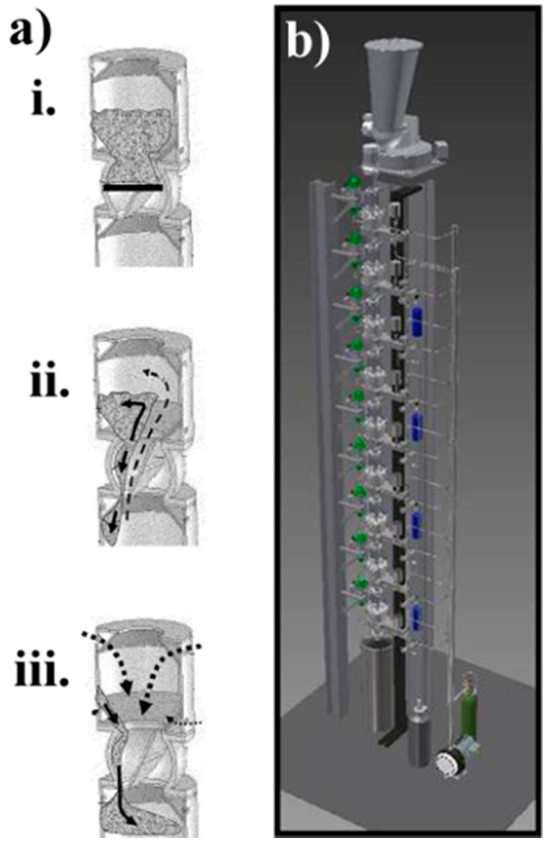

Figure 6. Schematic spatial ALD processes using powder reservoirs. (a) Schematic of powder reservoir theory of operation, i–iii. The powder to be coated is supported on a. (b) CAD drawing of a powder reservoir type reactor. Adapted from King et al. and material available in the public domain.[96,97]

preliminary results for depositing Pt nanoparticles on TiO_2.[99] In this configuration, a powder is moved using pneumatic transport through a winding tube made up of reaction zones that alternate between empty or purged regions.

An alternative approach to the agitation of particles during ALD is in the use of rotary bed reactors (Figure 5b).[50,51,88,91,100] In this approach, the powder is typically contained within a rotating cylindrical enclosure with porous walls through which the reactants diffuse. Remote plasma ALD has been demonstrated on powders in a rotary bed,[50,51] in which an RF coil on a rotating quartz tube is used to energize precursors before the gas reaches the catalyst support. The remote plasma source allows the higher-energy ions to recombine before impinging on the coating surface, where their interaction can lead to defects. Note that although the rotary reactor is simpler than alternatives such as spatial or fluid bed ALD, it is also more likely to waste precursor as a result of bypassing of the substrate in the reactor.

One of the primary hurdles for ALD catalysts is that the volatile precursors are often more expensive than the materials used in traditional synthesis, which means that ALD reactors must ensure maximal usage of the precursor. This point and the large powder-substrate-to-reactor surface area ratio achievable in a fluidized bed reactor (in combination with fact that scaled commercial processes for fluidization technology have already been developed) are the reasons that fluidized beds are often considered the preferred technology. It is worth noting that the disadvantaged cost of "rare" precursors is not an uncommon hurdle in commercialization of new materials (or other advanced technologies for that matter) as appropriate large scale applications for the precursor are required before large scale production is pursued, which can subsequently bring down the costs drastically. In addition, although continuous processes generally have advantages with respect to capital and operating labor expenditures, the fact that fluidized bed ALD is a batch process with respect to the catalyst should not necessarily be considered prohibitory because industrial scale catalyst manufacturing is commonly done via batch synthesis (e.g., zeolite crystallization).

Implementation of ALD catalyst manufacturing on a commercial scale will require integration into the existing manufacturing infrastructure, execution at an economically feasible cost, detailed reactor design, and process intensification. Since catalyst manufacturing costs represent the summation of materials costs, capital expenditure, and labor, some promising routes to reducing total costs include increasing reactor throughput (e.g., continuous operation via spatial ALD for efficient use of capital and labor), increasing precursor utilization (reducing materials cost), and reducing net energy consumption during operation (lower temperatures, reduced use of vacuum, etc.) Choosing the appropriate reactor will require finding the appropriate cost mitigation strategies with the required material specifications on a case-by-case basis and may be driven by the needs of individual applications. Although ALD on powders at a commercial scale is still not realized, these advances provide an expanding set of options for technology development.

3. ALD OF METAL OXIDE CATALYSTS

3.1. Fundamental Insight and Application of ALD Metal Oxides for Catalysis. Among materials deposited by ALD, metal oxides are perhaps the most predominant (Figure 1) because of their early applications as thin film insulators and semiconductors for microelectronics, their adherence to the traditional concept of AB ALD outlined in the previous section, and the relative availability and efficiency of the oxygen precursor source (e.g., water, O_2, O_3, alkoxides, etc.). For catalytic applications, the conformal deposition allows the creation of well-defined oxide catalysts over intricate morphologies with high surface area, such as common catalytic supports like mesostructured silica.[55,101−103] ALD on these supports effectively enables the synthesis of mesostructured oxides of any metal, with a high degree of control over pore size due to the atomic level control of ALD. From a catalytic standpoint, ALD of metal oxides has been used for the creation of catalytic sites and designed nanostructures and for depositing protecting overlayers on other catalytic materials.

Part of the prevalence of the application of metal oxide ALD in catalysis is that the deposition of metal oxides can utilize a wide range of metal−organic precursors, ranging from metal chlorides, β-diketonates, alkyls, alkoxides, and metallocenes, with oxide formation often being the most thermodynamically favorable product.[104] During the first cycle, the ligands on the metal precursors act as spacers that allow the chemisorption of isolated metal centers, which upon subsequent reaction leaves site-isolated metal oxides. Moreover, after the first cycle, the density of the resulting metal oxide is controlled by the bulkiness of the ligand,[105] the presence of blocking molecules on the surface,[79,106] the number of bonding sites on the support,[107] and the number of reaction cycles.[108,109] These examples are just some of the relatively large number of

DOI: 10.1021/cs501862h
ACS Catal. 2015, 5, 1804−1825

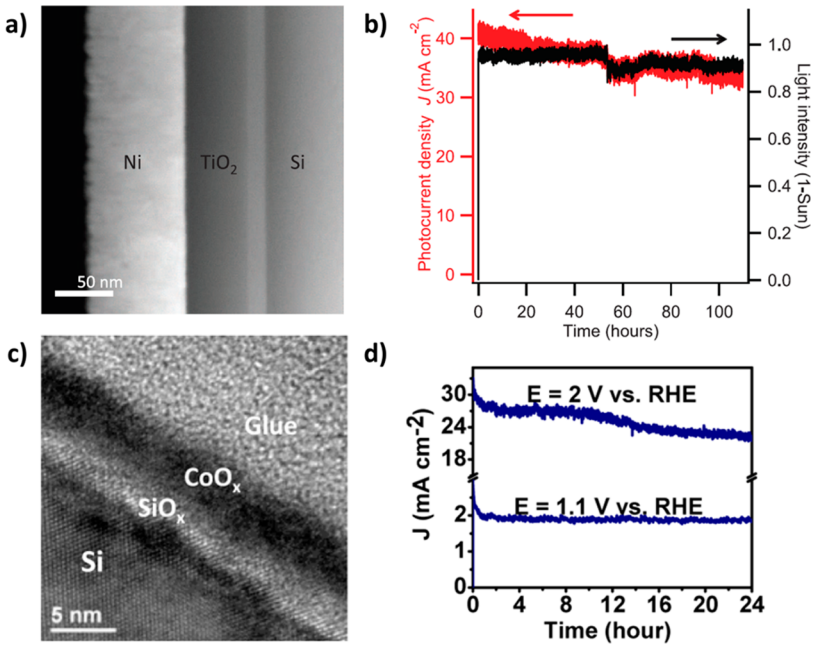

Figure 7. (a) STEM image of Si/ALD-TiO_2/Ni interface as a photoanode for water oxidation. (b) Chronoamperometry of the n−p^+-Si/ALD-TiO_2/Ni photoanode at 0.93 V versus SCE in aqueous 1.0 M KOH under 125 mW cm^{-2} of illumination intensity. (c) Cross-sectional TEM image of ALD-CoO_x/p^+n-Si photoanode. (d) Chronoamperometry of the ALD-CoO_x/p^+n-Si photoanode at 1.1 and 2 V versus RHE in aqueous 1.0 M NaOH under 100 mW cm^{-2} of illumination intensity. Parts a and b reproduced with permission from Hu et al. Copyright 2014, AAAS.[118] Parts c and d reproduced with permission from Yang et al. Copyright 2014, American Chemical Society.[127]

synthesis variables that can be controlled, allowing ALD to achieve such high degrees of atomic selectivity over such a wide range of materials. Furthermore, the gas phase deposition approach does not involve the solvents used in traditional wet or incipient wetness impregnation that often lead to aggregation of the metal centers as the solvent evaporates.

The atomic control of ALD over the growth of the metal oxide allows for the monitoring of the evolution of structure and its correlation with catalytic properties. This control is an important example of how ALD can be used as a tool to contribute to fundamental understanding. Among the most extensively studied systems are titania-[102,103,110−112] and vanadia-[103,112−115] supported catalysts. Titanium and vanadium oxide on SBA-15 and FDU-15 have been studied using liquid-phase cyclohexene epoxidation, and the catalytic activity has been observed to scale with the increasing amount of titanium and vanadium oxide deposited by ALD.[112] Importantly, the porosity of the SBA-15 and FDU-15 was maintained during the ALD process, demonstrating that ALD can be used to make catalytic sites over high surface areas with intricate morphology. In the case that a high surface area support is used, catalysts with larger active surface areas can be achieved with ALD coating than by synthesizing the corresponding bulk oxide. In another example, VO_x supported on nonporous SiO_2 and Al_2O_3 synthesized via ALD and impregnation demonstrated that catalysts prepared using ALD showed superior catalytic activity for propane dehydrogenation compared with impregnated catalysts.[111,115] A similar trend was observed for cyclohexane dehydrogenation using VO_x supported on anodic aluminum oxide (AAO) prepared using ALD and incipient wetness impregnation.[25] Low loadings of VO_x deposited by ALD showed monomeric oxo species, and it was observed that ALD-prepared catalysts were 2−7 times more active than the corresponding loading deposited by incipient wetness impregnation. The superior activity was attributed to the dispersion of the vanadium centers deposited by ALD onto AAO. ALD-derived metal oxide catalysts have demonstrated superior catalytic activity (compared with catalysts prepared by impregnation techniques) for epoxidation of cyclohexene,[112] *o*-xylene oxidation, oxidative dehydrogenation (ODH) of cyclohexane,[25] propane dehydrogenation,[115] and liquid-phase butanol dehydration,[103] primarily as a result of increases in catalytic dispersion and stability resulting from deposition of thin films on high-surface-area supports that prevent the active phase from crystallizing and sintering.

ALD also has been applied as protective coatings to impart stability for the underlying oxide, a topic discussed in more detail in Section 5. Coatings of niobia ALD have been used to hydrothermally stabilize both the acidic NbO_x film and the SBA-15 support.[55] Silica is widely used as a catalyst support; however, hydrothermal conditions, common in biorefining, lead to silica restructuring, which causes loss of surface area and catalytic activity. Deposition of NbO_x on SBA-15 consumes the surface silanols, thereby stabilizing the mesostructure of the SBA-15, even under the hydrothermal conditions. This stabilized material can then be used as a high-surface-area NbO_x catalyst or as a support (ALD for support modification discussed more in Section 4.1). By adding Pd on the deposited NbO_x, a bifunctional catalyst active for the conversion of γ-valerolatone to pentanoic acid was demonstrated. The synthesis of bifunctional catalysts is particularly important for areas such as biomass conversion, in which bifunctionality can improve selectivity by converting highly reactive intermediates that lead to catalyst fouling and loss of yield.

For photoelectrochemical (PEC) applications, TiO_2 has been used to protect photocathodes of Cu_2O[116] and photoanodes of ZnO,[117] Si,[118] GaAs,[118] and GaP.[118] In these examples, ALD was utilized to demonstrate how the material performance depended on atomic control of film thickness because the protective layer must fall within a narrow range for optimal

DOI: 10.1021/cs501862h
ACS Catal. 2015, 5, 1804−1825

performance. Thick films were detrimental to the performance, and films that were too thin did not impart the desired stability.

Electrochemical water splitting ($2H_2O(l) \rightarrow 2H_2(g) + O_2(g)$, ΔE = 1.23 V) has been identified as an important reaction for its potential as a producer of "green hydrogen".[119] This reaction typically occurs in highly corrosive environments (high and low pH, high bias, etc.) which provide a significant stability challenge for the alkaline electrolyzers, proton exchange membrane electrolyzers, or solid oxide electrolysis cells that are commonly used.[119] ALD has been used to add metal oxides to different semiconductor or metal catalysts to make anode and cathode catalytic materials with improved activity and stability for water electrolysis, photoelectrolysis, and photocatalytic water splitting (without a bias).[32]

Metal oxides are also common catalysts in photoelectrolysis and photocatalytic water splitting because they can reduce or eliminate the required bias, and ALD catalysts have made important contributions in the improvement of these catalysts. ALD is used to create materials with controlled thickness and composition and to investigate oxide interface chemistries. In one example, hematite (Fe_2O_3) is investigated for PEC splitting of water due to its abundance and desirable 2.1 eV band gap, which enables absorption of a significant fraction of the solar spectrum (up to ~580 nm);[120] however, the overall solar conversion efficiency of traditional hematite electrodes is poor. To improve the efficiency, hematite is synthesized via ALD, and other metal oxides such as Mg[121] and Ga[122] are systematically incorporated, utilizing the atomic control of ALD. The controlled Mg doping of hematite via ALD allows the creation of p-type hematite, which when deposited on top of an n-type hematite leads to an n−p junction that creates a built-in field that can be used to assist in PEC cells.[121] Other examples include the deposition of hematite on ALD deposited Ga_2O_3 and Nb_2O_5 underlayers over fluorine-doped tin oxide. The presence of Ga_2O_3 and Nb_2O_5 improves the crystallinity of the hematite compared with bare fluorine doped tin oxide.[120] The improved crystallinity decreases the density of defects, resulting in decreased recombination with the back contact. Other oxides being explored for PEC include WO_x[123] and MnO_x.[124] Tungsten oxide synthesized by ALD and paired with a manganese-based catalyst leads to the stabilization of WO_3 at pH 7 during PEC splitting of water.[123] Manganese oxide ALD on glassy carbon, which upon heat treatment yields Mn_2O_3, was also demonstrated as an excellent catalyst for the oxygen evolution reaction.[124]

Other important applications of ALD in this area of catalysts include photoanodes coated with a metal oxide ALD layer over the semiconductor surfaces.[118,125−127] It has recently been reported that ALD of a conformal TiO_2 layer protects a Si photoanode against corrosion.[125] The thin ALD TiO_2 layer allowed continuous operation in acidic and basic conditions in 100 mW cm^{-2} of simulated solar illumination at 5.1 mA cm^{-2} photocurrent density.[125] Very recently, as shown in Figure 7a,b, over 100 h of continuous operation at a current density of >0.30 mA cm^{-2} was demonstrated using an ALD TiO_2-coated Si photoanode in conjunction with Ni.[118] A Si photoanode was also stabilized during water oxidation using an ALD CoO_x coating. This coating made the Si photoanode (Figure 7c) corrosion-resistant while maintaining a high photovoltage (610 mV) for water oxidation at pH of 13.6.[127] Figure 7d shows the stability of the ALD-CoO_x-coated Si photoanode under simulated solar illumination (100 mW cm^{-2} intensity).[127]

ALD-deposited SrO_x, AlO_x, and CeO_x films on solid oxide fuel cell (SOFC) cathodes (35 wt % $La_{0.6}Sr_{0.4}CoO_3$, $La_{0.6}Sr_{0.4}FeO_3$, or $Ba_{0.5}Sr_{0.5}Co_{0.8}Fe_{0.2}O_3$ supported on yttria-stabilized-zirconia scaffolds) have been used to demonstrate the effect of ALD modification on the performance of the cathode for the oxygen reduction reaction (ORR).[128] ALD SrO_x, AlO_x, and CeO_x coatings decreased the oxygen adsorption ability of the cathode, thereby deactivating the cathode for the ORR. ALD SrO_x and AlO_x films blocked the active surface area of the electrode, whereas ALD CeO_x films preferentially interacted with oxygen vacancies on the surface of the electrode, increasing the impedance.[128] Through the ALD-modified SOFC studies, it was demonstrated that the oxide morphology, which can be more easily controlled with ALD, is important for modifying the performance of perovskite-based electrodes. In another example, it was reported that ALD ZrO_2 overcoating over a SOFC cathode ($La_{0.6}Sr_{0.4}CoO_{3-\delta}$ supported on $La_{0.8}Sr_{0.2}Ga_{0.83}Mg_{0.17}O_{3-\delta}$ scaffold) stabilized the $La_{0.6}Sr_{0.4}CoO_{3-\delta}$ particles and suppressed Sr segregation at the surface during operation at 700 °C for over 4000 h of continuous ORR operation.[129] In addition, the polarization area-specific resistance and degradation rate of the ALD electrode decreased by factors of 19 and 18, respectively, compared with an analogous non-ALD electrode.[129]

Catalysts synthesized by ALD have also been used for solar water splitting with visible light without using a bias.[130] A plasmonic photocathode was prepared that consisted of ALD TiO_2-coated gold nanowires capped with Pt nanoparticles. Three thicknesses of ALD TiO_2 film (8, 12, 21 nm) were studied, and it was concluded that an 8 nm TiO_2 thickness gave rise to the highest photocurrent (−18 μA cm^{-2}), another example of how the superior precision of ALD can be used to improve catalyst performance.[130] In another example, H_2 was produced via water splitting, with a high-temperature redox cycle using $CoFe_2O_4$ deposited on different substrates (Al_2O_3 or ZrO_2) by ALD.[131,132] It was shown that the ALD $CoFe_2O_4$/Al_2O_3-based water splitting, with isothermal redox cycle at 1623 K, generated over 6 times more H_2 than non-ALD ceria-based water splitting catalysts with traditional temperature-swing redox cycles.[132] The ALD $CoFe_2O_4/Al_2O_3$ was also effective for CO_2 splitting to CO and O_2 after reduction at temperatures 150 K lower than traditional iron oxide- and ceria-based materials.[133] In this example, the compositional control and improved interfacial area between the materials that was achieved by ALD was crucial to the improved catalytic performance.

The envisioned application for the H_2 that would be produced in the preceding examples could be for the production of electricity in fuel cells or the hydrogenation of CO_2. Methanol was produced via CO_2 reduction with water using ALD TiO_2-coated p-GaP photocathodes having different ALD TiO_2 thickness with the TiO_2 preventing corrosion of the GaP. In addition to stability, the ALD TiO_2 layer enhanced efficiency of the process by forming a pn-junction with the underlying GaP. The increase in the TiO_2 layer thickness from 1 to 10 nm led to the shift in overpotential from 0.1 to 0.5 V, demonstrating how ALD can be used to tune the final performance.[134] ALD has also been used to control the dispersion of metal nanoparticles (which is discussed in more detail in the next section) and metal loading for electrodes of proton exchange membrane fuel cells (PEMFCs).[23,135] The catalytic activity of Pt and the efficiency of PEMFCs depend on the Pt loading and its dispersion on the support materials, such

DOI: 10.1021/cs501862h
ACS Catal. 2015, 5, 1804−1825

as CNTs. It has been an important challenge to control Pt loading and dispersion on the support for PEMFCs. Previous methods to deposit Pt on the support have low productivity and high Pt loading. ALD not only provided uniform dispersion of the Pt on the CNTs but also allowed the Pt loading on the CNTs to be controlled from 0.02 to 0.10 mg cm^{-2} by changing the number of ALD cycles from 100 to 400 cycles, with the resulting ALD-synthesized Pt electrode having 11 times higher specific power density than commercial electrode.[23]

3.2. Challenges and Outlook. The importance of the interplay between structure and performance for catalysts is well-known, but despite significant advancements in the characterization of catalysts and catalytic processes, it is often challenging to achieve atomic level understanding of detailed structure−property relationships. Many industrial catalytic processes (e.g., oxidation/combustion, pollution remediation, acid catalysis/zeolites, etc.) involve a metal oxide as the active phase or as the support, but there are very few examples in the open literature in which the structure−property relationships have been elucidated in a generalizable way such that they can be used as a fundamental basis on which to design improved materials. Much of the challenge is due to advancements in controlled synthesis lagging behind analytical advancements, where many examples of atomic resolution have been demonstrated.

Atomic layer deposition is poised to close this gap, given its atomic control over the metal oxide thickness and composition. These two important features of ALD facilitate the development of catalyst fundamentals because the process can be coupled with powerful analytical techniques, such as Fourier transform infrared spectroscopy (FTIR),[48] electron microscopy,[11,136] X-ray absorption spectroscopy (XAS),[137,138] X-ray diffraction (XRD),[139] X-ray photoelectron spectroscopy (XPS),[113,140] quadrupole mass spectrometry (QMS),[141] and quartz crystal microbalance (QCM),[89,141] which allow in situ and operando characterization of catalytic structures and processes. Significant insight can be gained from the incorporation of an ALD system with a synchrotron X-ray source, which would enable in situ XAS and XRD experiments. To date, this type of in depth analysis is missing from many of the studies of ALD catalysts, in which the novel ALD materials are often simply compared with materials made by more traditional means without elucidating the reasons for the altered performance. The stepwise, bottom-up approach of synthesizing metal oxides via ALD enables the observation of how the oxide structure evolves from an isolated metal-oxo species into its bulk form, and by manipulating the conditions of the synthesis, it is possible to probe the mechanisms of defect formation and elimination as well as probe the controlling variables that determine crystallinity. The capabilities of ALD enable studies to address fundamental problems, such as when a metal oxide starts to exhibit bulk properties, what the nature of the Lewis and Bronsted acid structures in amorphous silica−alumina are, and how these properties depend on the local environment. Moreover the "digital" nature of the synthesis virtually eliminates variations that can arise from sample handling and preparation.

Although ALD holds great promise in catalyst synthesis and in understanding fundamentals of catalysts and catalytic processes, important challenges remain. As mentioned previously, a deeper understanding of structure−property relationships is necessary for the optimization and improvement of current catalysts. ALD-derived metal oxide catalysts often outperform catalysts derived from traditional approaches, such as impregnation and precipitation, in terms of at least one of the three important aspects of catalyst performance (activity, selectivity, and stability); however, despite the potential, shifting catalyst synthesis away from the traditional techniques is hindered by the scalability and cost of current ALD technology for catalyst synthesis. In addition to eventual advancements in ALD reactor design, the ability to build catalytic sites with superior performance using less cycles of ALD should help to offset the cost. However, further lab scale demonstrations of proofs-of-concept showing superior catalytic properties of ALD-derived catalysts are needed to continue motivating research on scale−up of this technology for catalysis.

4. ALD FOR SUPPORTED METAL CATALYSTS

4.1. Support Modification and Synthesis. Although ALD oxide films can be deposited and directly used as catalysts, as was discussed in the previous section, the conformal nature of metal oxide deposition by ALD makes it possible to prepare a high-surface-area catalyst support, with a tunable pore size, composed of any ALD-deposited thin film by simply coating a conventional high-surface-area platform, such as SiO_2 or Al_2O_3. Alternatively, more unconventional sacrificial templates, such as polymer, may be used as well.[142] Other, atypical platforms, such as catalytic nanoliths, single crystals, and nanoporous bulk metals such as gold can also be prepared as supports using this approach.[25,39,143] Because most of the catalytically interesting metal oxides can be deposited by ALD (e.g., TiO_2, Al_2O_3, ZrO_2, CeO_2), the ability to make practical supports of these oxides considerably expands the scope of possible catalyst materials. Synthesis of even high-surface-area, multicomponent mixed oxide supports should be possible. Although the support is not often considered to be directly involved in the catalysis, there exist innumerable applications in which the nature of the support does have significant implications in catalyst performance, and the ability to systematically vary the nature of the support via ALD should help provide valuable insight into the role of the support materials.

An interesting example of support synthesis by ALD and its impact on catalysis can be found in work studying support effects in liquid-phase reforming of 1-propanol by supported Pt.[144] The catalysts were prepared by coating nonporous NanoDur spherical alumina with 20 ALD cycles of TiO_2 or CeO_2, followed by deposition of Pt using 1 ALD cycle. In this way, observed differences in reaction kinetics can only be due to the change in the support surface because surface area, porosity (in this case, none), and metal deposition were the same for all of the catalysts. In a comparison of the two ALD-coated samples with the catalyst prepared by deposition of Pt directly on the NanoDur, TEM analysis showed that the Pt particles deposited on the TiO_2 and CeO_2 deposits were significantly smaller and possessed a narrower size distribution. After reaction, the particle size had increased, but the Pt particles were measurably larger when using the bare alumina support than they were with supports consisting of TiO_2 or CeO_2 ALD thin films. This behavior was a convincing indication of a stronger interaction between the Pt and CeO_2 and the Pt and TiO_2 supports. In addition, the Pt/TiO_2 also showed twice the activity of the catalysts using alumina or ceria supports, more than could be accounted for based on increased dispersion alone, suggesting the support does more than provide surface area for dispersion.

DOI: 10.1021/cs501862h
ACS Catal. 2015, 5, 1804−1825

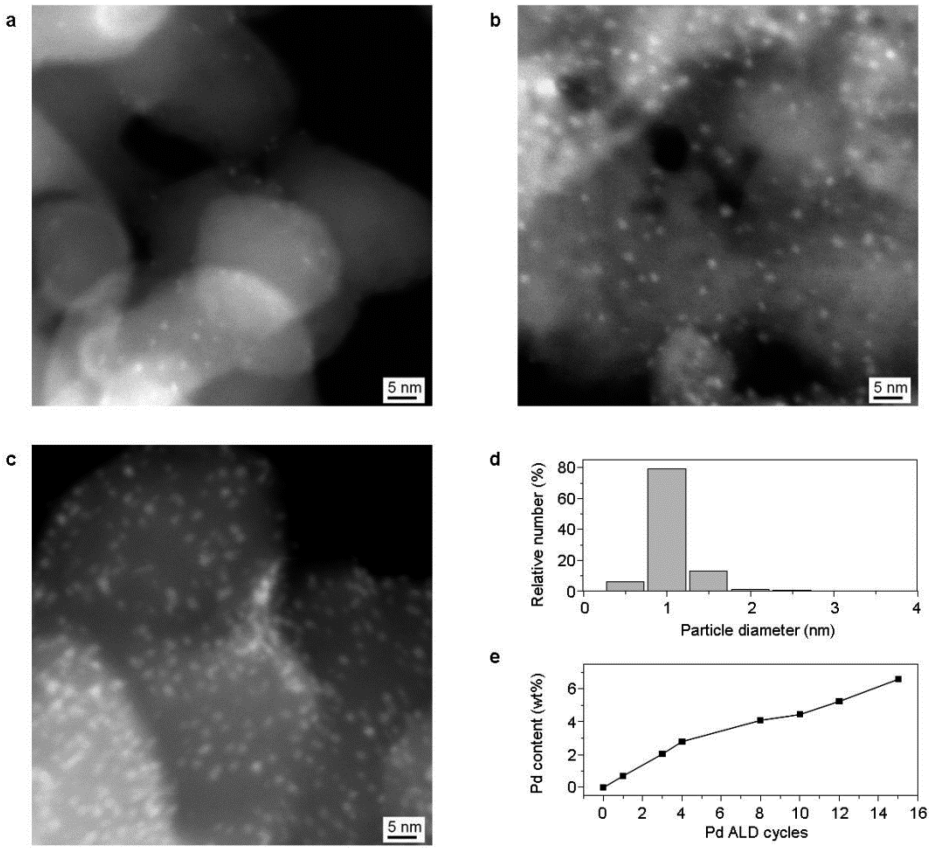

Figure 8. STEM images of (a) 1 ALD cycle of Pd on AlO_x-coated SiO_x, (b) 4 ALD cycles of Pd on AlO_x-coated SiO_x, and (c) 15 ALD cycles of Pd on AlO_x-coated SiO_x. (d) The particle size distribution of 15 ALD cycles of Pd on AlO_x-coated SiO_x and (e) the measured metal loading as a function of Pd ALD cycles demonstrate the exceptional control of particle size available by ALD. Figure reproduced with permission from Lu et al. Copyright 2010, John Wiley and Sons.[39]

A solution-phase analog to the gas phase ALD support modification has been demonstrated for rhenium oxide-catalyzed 2-butanol dehydration.[145] In this study, ReO_x supported on mesoporous silica (SBA-15) is compared with the same support modified by alumina, deposited from toluene and ethanol solution using aluminum isopropoxide. ReO_x on the pure silica support exhibited the highest initial activity but showed significant deactivation after ∼2 h of reaction. The activity of the catalyst using the alumina-modified silica support was lower initially, but better maintained its activity. After 3 h, the catalyst with the modified support had higher activity than the materials using pure silica. Strong interactions between the ReO_x and the alumina were inferred from ^{27}Al NMR, which suggested bonding between rhenium oxide and acidic 5-coordinate aluminum, elucidating the way that ReO_x anchors to the support, and ac-HAADF STEM, which showed improved resistance to sintering and the formation of raft-like structures on the alumina-modified silica.

4.2. Monometallic Nanoparticle ALD. Like much of the pioneering work on ALD, the potential to better control the composition, density, and size of supported metal catalysts was first described in a Finnish patent from the group led by Tuomo Suntola at Microchemistry Ltd. in 1992[146] and later described in an article by Lakomaa from the same group.[147] The concept of controlling the particle size by preparing the support with appropriate ALD layers, by the nature of the metal precursor, and the reaction temperature were all contained therein. The deposition of Cr was one of the examples cited, and the concept is also summarized in a review by Ribeiro and Somorjai in 1994.[148]

To the best of our knowledge, the earliest report of a supported metal catalyst prepared by ALD in the open literature (referred to as ALE in the publication, and excepting early Soviet work on ML published only in Russian) was nickel on alumina prepared using $Ni(acac)_2$ and air as the A and B reagents, respectively.[108] This report was issued at nearly the same time as the review by Ribeiro and Somorjai.[148] The catalyst activity for toluene hydrogenation was determined for a series of materials with increasing Ni content obtained by increasing the number of ALD cycles. The catalyst showed no activity after the first cycle, but the activity per gram of Ni increased with loading, passing through a maximum before declining. This behavior is similar to Ni/alumina materials prepared by conventional methods and is attributed to the catalytic requirement for metallic nickel, which is formed only when nickel ensembles of sufficient size are present.[149] As compared with other supported metal NP systems described later, the ALD deposited nickel in the Ni/Alumina material deposits in a cationic form, and when the loading is sufficient, reduces to metallic Ni under the reducing conditions of the toluene hydrogenation. This example illustrates how the extraordinary control of the metal nanoparticles can help to elucidate the nature of the catalytic active site. More recently, nickel supported on silica catalysts for dry reforming of methane were prepared by ALD.[150] Compared with traditional methods of preparation, the ALD materials were characterized

DOI: 10.1021/cs501862h
ACS Catal. 2015, 5, 1804−1825

by much higher dispersion and more uniform particle size. These materials exhibited better performance for methane reforming than unsupported NiO materials in terms of selectivity and stability against coke formation.

An ALD process to prepare supported palladium nanoparticle catalysts has been demonstrated and studied for methanol decomposition.[67] The process makes use of Pd(II) bishexafluoroacetylacetonate ($Pd(hfac)_2$) as the metal precursor (A reagent) and formalin, a mixture of methanol and formaldehyde, as a reducing agent (B reagent) to form metallic palladium.[151] Two supports, ZnO-coated silica gel and Al_2O_3-coated silica gel, were employed. The ALD process produced highly dispersed, highly uniform Pd particles with dimensions of 1−2 nm. Further work to tune the Pd particle size explored the role of reaction temperature and blocking of surface hydroxyl groups using reaction with ethanol or trimethylaluminum.[74] It was found that by lowering the ALD growth temperature from a typical value of 200 to 100 °C, the Pd particle size distribution narrowed, with an average size of 0.8 nm (SD = 0.2 nm) and approximately the same loading as produced by the higher temperature growth.[67] The TOF observed from the smallest particles was ∼2 times that of larger, 2 nm Pd particles. Similarly, the space time yield of hydrogen production from methanol decomposition was 2 times that of a conventional Pd/alumina catalyst prepared by incipient wetness impregnation of $PdCl_2$.[152] This example illustrates how ALD can be used to obtain the practical goal of increased dispersion and activity while simultaneously helping to elucidate catalytic fundamentals such as structure sensitivity of a reaction through careful control of the particle size.

In addition to Pd, ALD preparation of catalyst materials containing Pt,[153−156] Rh,[153] Ru,[153,157] Ir,[153,158,159] and Ag[66] on supports ranging from carbon, silica, alumina, and titania have been described, among others, representing most of the catalytically interesting late transition metals. In addition to Pd, characterization of particle size and study of the growth mechanism have been performed for Pt,[39,154] Ir,[158] and Ag,[66] with the majority of catalytic experiments having been conducted using materials containing supported Pt and Pd. Generally, the nanoparticle size depends primarily on the deposition temperature and the number of deposition cycles. Nanoparticles in the range of 1−3 nm with small deviations (Figure 8) are typical of most metals, although with Ag, the size is larger. The catalytic reactions that have been studied over these materials include methanol decomposition,[67,74] oxidative dehydrogenation,[10,160] propane combustion,[5] and CO oxidation.[156] In addition, tandem reactions have been described for liquid-phase ether hydrogenolysis by a lanthanide triflate and supported Pd combination, an important reaction for the potential utilization of lignin,[161] and for an enzyme and supported Pd combination used for stereoselective transformations potentially useful in the pharmaceutical industry.[162]

Most heterogeneous catalysts are synthesized with techniques or supports in which atomic scale control and characterization of multiple components at the catalytic surface is difficult.[163] This difficulty leads to considerable uncertainty about the surface composition and atomic arrangement and is a major impediment in understanding catalytic performance at the atomic scale and designing improved materials. The uniformity of supported nanoparticle size achieved with ALD provides the means to overcome one source of inhomogeneity in solid catalyst materials. When combined with highly uniform, crystalline support materials, this aspect of ALD nanoparticle synthesis provides the opportunity to investigate the interactions between supports and metals with atomic detail. One such combination has been the study of Pt nanoparticles on single crystal $SrTiO_3$ (STO) nanocuboids. The STO support, when prepared under the proper conditions using hydrothermal synthesis, adopts a cuboidal nanoparticle shape with dimensions in the range 10−100 nm and facets in the (001) surface orientation.[164] Furthermore, it is possible to control whether the facets are terminated by TiO_2 or SrO layers. Nanoparticles of Pt (or any metal) supported on the facets have shapes that are thermodynamically controlled according to the so-called "Winterbottom construction,"[165] which is analogous to the Wulff Construction[166] but includes the interfacial free energy between metal and support. In a demonstration of the control of the formation and growth of nanoparticles, high-resolution electron microscopy was used to show that the supported ALD-Pt nanoparticles adopt the Winterbottom construction.[136] Essentially, the nanoparticles appear with the Wulff shape truncated by the plane of the support. The orientation of the truncation plane depends on the epitaxy between metal and support, which for Pt and STO is cube−cube. When the support composition changes from $SrTiO_3$ to $Ba_{0.5}Sr_{0.5}TiO_3$, the lattice mismatch energy increases, as does the corresponding interfacial energy, as evidenced by the appropriate shift in the truncation plane.[167] When used in the catalytic hydrogenation of acrolein, Pt supported on $SrTiO_3$ was more selective for the allyl alcohol product, as expected for nanoparticles with the Winterbottom construction because of their higher proportion of (111) facets. This demonstrates a predicted structure−function relationship that was proven by experiment. This result would not have been evident or as convincing without the uniformity of particle size, and consequently active sites, obtained from the ALD synthesis that leads to an essentially ideal model catalyst. Further insights and experimental proofs can be anticipated in the future with the application of this strategy to other systems or with the use of ALD oxide overcoats on supported metal nanoparticles, as described later.

4.3. Bimetallic Nanoparticle ALD. The addition of a second metal component to a supported metal nanoparticle catalyst provides an additional level of flexibility and complexity. Not only are there variations in particle size and shape with which to contend, but also variations in particle composition and elemental arrangement of the metals into core−shell or intimately mixed structures. This flexibility and complexity, however, leads to significant inhomogeneity in catalysts synthesized by traditional techniques. This in turn has significantly hindered the fundamental understanding of the nature of the active site in bimetallic catalysts and limited the rational development of improved materials. The capability to prepare uniform catalytic materials by ALD significantly reduces this variability and facilitates the ability to understand the experimental catalytic results they produce.

The preparation of bimetallic nanoparticles on high surface area supports using ALD has been demonstrated for PtRu,[6,8] PdRu,[8] and PtPd[8,9] systems. A primary goal of the synthesis strategy is to prepare materials with exclusively bimetallic nanoparticles and no monometallic nanoparticles. With the proper selection and sequence of reactions, it is possible not only to meet this goal but also to controllably form core−shell or well mixed bimetallic nanoparticles with a given pair of metals. An example of what can be achieved is presented for the PtPd system (Figure 9).[8,69] The strategy is to deposit the two

DOI: 10.1021/cs501862h
ACS Catal. 2015, 5, 1804−1825

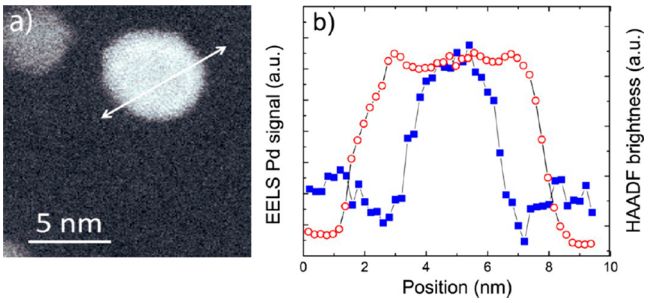

Figure 9. EELS line scan across a single Pd/Pt nanoparticle. (a) The position of the line scan is indicated in the HAADF-STEM image. (b) Only Pd (blue squares) could be detected by EELS because the Pt signal appeared to be too weak. The HAADF brightness profile (red circles) displays the full diameter of the particle (~5.5 nm). The Pd signal was detected only in the core (~3.5 nm wide) of the particle. Figure reproduced with permission from Weber et al. Copyright 2012, American Chemical Society.[69]

metals sequentially at a low reaction temperature where the rate of deposition on the oxide is slow compared to the rate of deposition on previously deposited metal nanoparticles. Thus, core−shell nanoparticles of the type Pd@Pt (Pt core, Pd shell) and Pt@Pd (Pd core, Pt shell) are formed by simply changing the sequence in which the two metals are deposited at 150 °C: $MeCpPtMe_3-O_3-n[Pd(hfac)_2-H_2]$ and $Pd(hfac)_2-HCHO-n[MeCpPtMe_3-O_2]$, respectively. In the first case, Pd selectively deposits on the Pt when H_2 is used as the B reagent. Likewise, Pt deposits selectively on Pd when O_2 is the B reagent. The number of cycles used for each metal, *n*, is chosen depending on the desired particle size and thickness of the shell.

A more subtle strategy is required to deposit well-mixed PtPd alloy nanoparticles using an ABC ALD approach. In this case, the sequence is $MeCpPtMe_3-O_2-H_2-Pd(hfac)_2-H_2-O_2$. The 6-step sequence is then performed through a number of cycles, depending on the desired size of the nanoparticles. The H_2 treatment prior to $Pd(hfac)_2$ converts the Pt oxide shell to the metallic state, which enhances Pd deposition. The O_2 treatment at the end of the sequence, prior to $MeCpPtMe_3$, forms the oxide skin, which is the preferred reaction surface for the Pt precursor. Both ac-HAADF STEM images and CO FTIR measurements demonstrate that the nanoparticle growth proceeds as desired.[8] In addition, simple catalytic tests using propane ODH over PtPd[9] and methanol decomposition over PtRu[6] bimetallic nanoparticles demonstrate enhanced activity when compared with the physical mixture of the two monometallic catalyst materials.

4.4. Challenges and Outlook. The ability to achieve atomic control of the size, density, composition, and structure of monometallic and bimetallic nanoparticles makes ALD an exceptionally powerful tool for catalysis research. Furthermore, it is an excellent way to maximize the benefits of high surface area supports, with ALD deposition having been demonstrated on metal organic frameworks,[168] aerogels,[156,169] zeolites,[57] carbon nanotubes,[22,23] and graphene.[170] The investigation of controllable parameters involved in the deposition processes (such as choice of reagents, temperature, and flux) is in its infancy. Continually expanding the flexibility of the ALD technique by widening the potential precursors, conditions, and resulting materials should be considered a primary goal, but searching out applications for the new catalyst materials and carefully elucidating why ALD materials perform better (or worse) at an atomic level rather than simply comparing the catalysts is at least as important. Expanded synthesis flexibility will allow for better elucidation of catalyst active sites as well as improved yield of the desired active site during catalyst synthesis. With continued improvements and understanding of the ALD chemistry, longstanding fundamental questions concerning structure sensitivity, the atomic structure of active catalytic sites, the site composition, and the dynamics of these properties under reaction conditions will be much more readily answered with highly uniform catalysts made possible by ALD. The synthesis of these controlled materials is especially critical for drawing conclusions from bulk characterization techniques, such as XAS, which rely on an assumption of uniformity (an assumption that is often downplayed and likely not met in many characterization studies of bimetallic materials). The potential control over nanoparticle size, composition, and shape, provides ALD the potential to be transformational in terms of how fundamental heterogeneous catalysis research is performed, helping to bridge the gap between molecular catalysts and heterogeneous catalysts by narrowing the distribution of possible active sites in a material and providing unprecedented control over the chemical properties and electronic structure of the nanoparticles.

5. NANOPARTICLE ALD OVERCOATING FOR CATALYSIS

5.1. Overcoating Metal Nanoparticles. An area of ALD application in catalysts conceptually related to bimetallics is the overcoating of supported catalysts. Whereas the creation of bimetallic catalysts relies on the atomically selective potential of ALD to deposit the second component so that it is chemically associated with only the first, overcoating leverages the ability of ALD to create conformal films over the high aspect ratio surfaces that result from depositing nanoparticles onto porous supports.

The first demonstration of utilizing fluidized bed ALD to coat particle surfaces was the use of TMA to deposit AlO_x films on boronitride particles,[171] and the demonstration of ALD on metals was soon to follow with the deposition of AlO_x onto Ni particles.[172] Although these early examples were not applied as catalysts, the demonstration of ALD coating of particles was an important technical development. The idea and successful demonstration of overcoating metal nanoparticles did not originate with the use of ALD. In fact, it was predated by different methods, including sol gel, precipitation, and CVD techniques that have been highlighted by others[173,174] (and references within) and is conceptually similar to the effects of strong metal support interactions.[2,175] However, these techniques have the significant downside that they often result in relatively thick, porous, and agglomerated overcoating films with little control over the resulting properties, whereas it has been shown that primary particles can be coated with controlled, nanothick, and initially pore-free ALD films.[176] The advantage of ALD that was realized in these early examples was the atomic level control that the technique provides, with subnanometer control over film thickness being orders of magnitude better than more primitive techniques. In addition, the conformal nature of ALD enables the synthesis of more homogeneous materials with a decreased number of film defects.

Figure 10 illustrates four strategies (types I−IV) that have been used to date to modify supported metal nanoparticle catalysts using ALD overcoats. In these examples, the support

DOI: 10.1021/cs501862h
ACS Catal. 2015, 5, 1804−1825

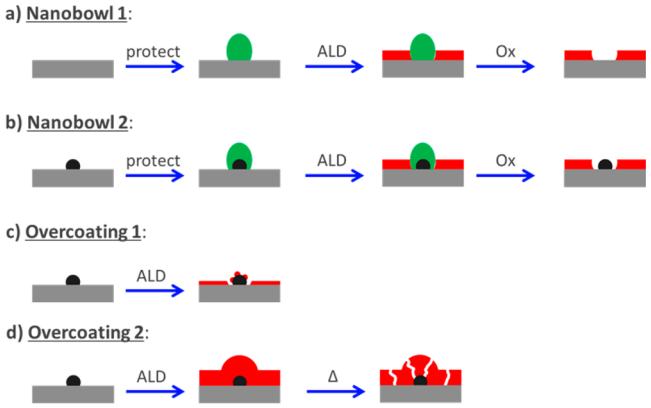

Figure 10. Four strategies for modifying supported metal nanoparticles using ALD overcoatings: (a) type I, nanobowl synthesis; (b) type II, metal nanoparticles isolated in nanobowls; (c) type III, selective decoration of nanoparticles; and (d) type IV, complete overcoating, followed by heating to induce nanoscale porosity. Gray represents the support material, black represents a metal nanoparticle, red represents the ALD overcoat, and green represents a removable grafting or template molecule.

(typically a hydroxylated metal oxide surface) is represented by the gray rectangle, the nanoparticle is the black circle, and the ALD coating is the red layer. In type I (Figure 10a), the active phase is first protected by grafting a molecular species (green) intended to block or inhibit the subsequent ALD process to prevent growth. For instance, the protecting species can be a bulky organic moiety, such as a calixarene or adamantanecarboxylic acid. Next, atomic layer deposition is performed to deposit a film, but the resulting layer grows only on the support surface and not on the blocking group. Finally, the blocking group is removed, for example, by oxidation using ozone, oxygen radicals, or by heating in O_2. The net result is a "nanobowl" with radius dictated by the size of the blocking group and depth determined by the thickness of the ALD layer.

In type II (Figure 10b), a metal nanoparticle can be isolated at the bottom of a nanoparticle by choosing a blocking or protecting group that selectively and strongly binds to the metal nanoparticle, such as hexafluoroacetylacetonate. In many cases, the blocking group could also be the original ligands of the metal precursor. These nanobowls can protect the nanoparticle against sintering and also provide size and shape selectivity to the catalyst.

In Type III (Figure 10c), the supported nanoparticle is subjected to a small number of ALD cycles (typically 1−10) such that both the nanoparticle and the support become at least partially coated but the film is intentionally discontinuous on the metal. The ALD coating on the support serves to stabilize the particle against agglomeration while the material deposited on the nanoparticle surface can inhibit coking, tune the catalytic selectivity, and reinforce weakly held low-coordination sites on the surface. These effects derive from selective growth of the ALD material on certain crystalline sites on the metal nanoparticle (such as defects, edges, and high index planes), leaving other sites uncoated (such as terraces and low index planes) and, therefore, available for catalysis.

In Type IV (Figure 10d), both the metal and support are completely overcoated with an ALD film several nanometers thick. In this state, the catalytic activity of the nanoparticle and substrate are completely eliminated since it is not possible for any compound to access the active surface. However, heating the sample densifies the ALD layer and induces nanoscale porosity that restores access to the nanoparticle surface. The net effect of this procedure is that the metal nanoparticle is protected against sintering and dissolution by the thick coating, but catalytic activity is achieved via the pores. Moreover, the size of the pores may be controlled by the temperature and duration of the heat treatment to introduce size or shape selectivity similar to a molecular sieve. Reordering of the ALD layer on the metal surface can preferentially expose certain sites on the nanoparticle surface (similar to Figure 10c) to further modulate the catalyst selectivity. In the future, it is possible and even likely that variations and extensions of these four types of ALD overcoating will be demonstrated.

One example of type I overcoating is demonstrated in the use of TiO_2 nanoparticle photocatalysts. By grafting of a calixarene template onto the TiO_2 nanoparticle, part of the TiO_2 surface was protected during subsequent ALD of an AlO_x overcoat.[79] Following ALD, the template could be removed, leaving behind a nanobowl that exposed at its bottom the photoactive TiO_2 (with size controlled by the size of the template employed, see Figure 10a). Using this method, the size selectivity of the photo-oxidation of substituted alcohols could be improved by nearly an order of magnitude. Similarly, by using the correct protecting groups, supported metal nanoparticles could be isolated at the bottom of similarly synthesized nanobowls, providing the ability to add size selectivity to the catalyst as well as provide a physical barrier to sintering via nanoparticle agglomeration (Figure 10b).[177]

Covering the surface of a catalytic metal nanoparticle by a thick ALD coating can lead to the loss of catalytic activity;[100] however, numerous methods have been developed that allow for selective re-exposure of the nanoparticles underneath.[174] One such method utilizes the exceptional thickness control of ALD to deposit submonolayer films (type III, Figure 10c). By controlling the bulkiness of the precursor ligands to physically space out the deposited precursors or by detuning the ALD synthesis parameters to achieve lower growth rates, films with coverages far below a monolayer can be produced. Furthermore, in some cases, the ligands of the ALD precursors can poison the ALD substrate, blocking the sites for precursor adsorption and limiting the amount of precursor deposited. This situation was utilized in the deposition of AlO_x onto Pd nanoparticles used to catalyze the decomposition of methanol.[178] In addition, this application demonstrated the benefit of ALD overcoating because despite blocking some of the active sites of the Pd nanoparticle, the ALD prevented the sintering of the catalysts, which actually had the effect of increasing the rate at longer times.[10,11,178]

By initially sacrificing part of the exposed active surface area, similar overcoating approaches have also been utilized to stabilize precious metal nanoparticles and preserve more of the active surface area in the long term. One such approach that has been demonstrated is the use of MLD overcoats consisting of alternating cycles of TMA and ethylene glycol over supported Pt nanoparticles.[14] After a thick shell of the MLD overcoat is deposited, the carbonaceous component can be removed by calcination, leaving behind a porous shell that re-exposes the Pt underneath. Further demonstrating the potential high degree of control of ALD or MLD, the resulting size of the pores in the overcoat can be manipulated by altering the carbonaceous precursor.[179] The use of larger precursors results in a larger pore size, imparting a tunable degree of size selectivity to supported metal nanoparticles (type IV, Figure 10d).

DOI: 10.1021/cs501862h
ACS Catal. 2015, 5, 1804−1825

The most commonly employed method for re-exposing the overcoated active phase is through thermal treatment (type IV, Figure 10d). As examples, this method has been utilized for ALD coatings on Au for CO and H_2 oxidation[100] and on Pd for oxidative dehydrogenation of ethane.[10] This method does not require organic precursors like MLD, potentially simplifying the synthesis, and it can be utilized to provide porosity even in relatively thick overcoat films. This approach is important because while in many cases thinner overcoats will be preferred to maximize rates per gram and minimize loss of active surface area, it is possible to envision scenarios where it is desirable to utilize the overcoat for additional applicability, as discussed later. In such cases, thicker overcoats could potentially offer offsetting benefits. The AlO_x overcoated Pd catalyst system was also key in the development of fundamental understanding of how the ALD overcoats interact with nanoparticles. Using FTIR spectroscopy and DFT calculations, it was shown that the deposited ALD precursors would selectively interact with the high-energy, low-coordination surface sites of metal nanoparticles.[4,10] These sites are believed to be responsible for the sintering and leaching phenomena that lead to irreversible catalyst deactivation.[180] The ability to selectively protect the most susceptible sites with atomic precision, while maintaining the catalytic activity of the rest of the nanoparticle is a primary example of what makes ALD such a potentially powerful catalyst synthesis technique.

Another useful application of ALD coating is the stabilization of base metal catalysts such as Cu,[11−13,138,181] Co,[16] and Ni,[17,182] which are prone to irreversible deactivation like such as and leaching, especially in the liquid phase, which is critical for applications in future biorefineries. There are instances in which these less expensive catalytic materials can perform the same chemistry as their more expensive precious metal counterparts; however, they deactivate quickly and become impractical alternatives.

The demonstration of nanoparticle stabilization of base-metal nanoparticles by ALD was done with a $Cu/\gamma\text{-}Al_2O_3$ catalyst overcoated with AlO_x, which was used for the hydrogenation of furfural in the liquid phase.[11−13,138] AlO_x overcoats on $CuCrO_4$ were also used to stabilize catalysts for the hydrogenation of furfural in the gas phase.[181] This reaction is industrially important, with over 250 000 tons of production per year over copper catalysts.[183] These examples of ALD overcoating of copper were an important breakthrough for the concept of stabilization of nanoparticles because it generalized the technique (precious and base metals) and the conditions in which it could be applied (high temperature gas and liquid phases). The fundamental knowledge about the interactions between the overcoat and the nanoparticle were extended from the prior work on the $Pd/\gamma\text{-}Al_2O_3$ catalysts. Subambient FTIR and scanning tunneling microscopy were used to demonstrate the atomic selectivity of ALD, showing the selectivity for initial deposition on low coordination sites and maintenance of that selectivity for low coordination sites after exposure to high temperature thermal treatments to open porosity in the overcoat.[11] An examination of how the overcoat changes to become porous while maintaining its stabilizing interaction was also probed with XRD and solid state NMR, suggesting that formation of small crystallites in the amorphous ALD films play an important role in pore formation.[11] Finally, in a first of its kind measurement, liquid-phase operando XAS measurements were used to measure particle sintering simultaneous to kinetics measurements to elucidate mechanisms of catalyst deactivation for liquid-phase furfural hydrogenation over $Cu/\gamma\text{-}Al_2O_3$ throughout its time on-stream and during catalyst regeneration.[138] The $Cu/\gamma\text{-}Al_2O_3$ system is an example of how ALD can be used to advance practical objectives (improvement of base-metal catalyst stability) as well as develop fundamental scientific knowledge (ALD film/nanoparticle interaction and mechanisms of $Cu/\gamma\text{-}Al_2O_3$ deactivation in the liquid phase).

The generalization of utilizing ALD to stabilize nanoparticles has continued as researchers have extended the applicability of the technique. TiO_x overcoating on Co particles was used for furfuryl alcohol hydrogenation, demonstrating the use of oxides other than AlO_x.[16] This work highlighted an important challenge as well as a strength of ALD overcoating. The combination of AlO_x overcoats with Co nanoparticles were shown to form a catalytically inactive cobalt aluminate phase after exposure to relatively moderate temperatures. This example underscores the challenge of materials compatibility between the overcoat and the nanoparticle and highlights an area where significant potential for rational design led by techniques such as DFT exists. Further generalization of ALD overcoating has been demonstrated by overcoating TiO_2 on Ni nanoparticles to reduce coking[182] and MLD of alucone to stabilize Ni for the dry reforming of methane.[17]

5.2. Functionalizing Overcoats. An emerging area of investigation is learning to manipulate the atomic control of ALD to further utilize the overcoat by imparting additional functionality to it. An early example of the overcoat having a functional role was its use to optimize photonic effects in TiO_2 photocatalysts by ALD coating Ag nanoparticles with atomically controlled thickness.[184] The atomic control was necessary both to elucidate the dependence of the photonic effects on spatial distribution and to create a material with optimized properties. Another example included the introduction of NbO_x overlayers with a protecting AlO_x overcoat on Cu nanoparticles to create a bifunctional catalyst.[12] This proof-of-concept example demonstrated how ALD can be used for process intensification by combining two reactions into one catalyst. The approach could be especially important when one of the reactions creates a highly reactive intermediate that can lead to carbonaceous deposits on the catalyst, a common occurrence in biomass refining. The addition of bifunctionality can ensure that the highly reactive intermediate is converted to a more stable product before its concentration is allowed to accumulate. Alternatively, rather than the addition of bifunctionality through the introduction of an additional active site, moderation of undesired overcoat activity through control of the overcoat thickness or composition has also been demonstrated. In this example, it was shown that decreasing overcoat thickness could decrease deactivation while increasing rate of furfural hydrogenation by decreasing the number of acid sites in the overcoat that lead to furfural resinification and pore blocking.[13] Building on that success, it was also shown that the controlled addition of basic MgO_x into an AlO_x overcoat could further reduce the number of acid sites in the overcoat, further decreasing the rate of deactivation.[13]

5.3. Outlook and Challenges. ALD overcoating has demonstrated remarkable selectivity toward deposition on high-energy, low-coordination sights on nanoparticle surfaces. Thus, ALD can be used to design more selective catalysts for reactions in which undercoordinated active sites catalyze unfavorable side reactions, as was shown for Pd and Ni catalysts on which coking side reactions were reduced after the introduction of ALD or MLD overcoats.[10,17] Perhaps more

DOI: 10.1021/cs501862h
ACS Catal. 2015, 5, 1804−1825

importantly, for reactions in which the mechanistic understanding is not as well understood or has not been experimentally verified, ALD can be used to synthesize selective nanoparticles in which the defect and low coordination sites have been eliminated by the use of ALD overcoating with a material that is inert for the chemistry under study.[185]

ALD overcoating would also be a powerful tool for examining mechanisms in which the support is suspected to play a significant role. ALD could be used to completely cover the support before deposition of the nanoparticles, changing the support chemistry without significantly altering the final morphology. The same approach could also be used to synthesize inverse catalysts that would result in an increased number of sites where metal and support material are in intimate contact.

As highlighted above, ALD overcoating provides numerous opportunities for practical solutions as well as scientific insight. However, many challenges remain to be addressed. One particularly important issue that was mentioned previously is the issue of materials compatibility.[16] Materials need to be chosen that will ensure either proper segregation or intermixing at the interface, depending on the application of choice. Although there is significant prior art in this area from materials science and metallurgy, more study is needed to understand how this knowledge transfers to the atomic scale. To leverage the advantages of atomic selectivity and precision provided by ALD, the interfacial integrity must be strictly maintained, as opposed to the case of thick films and bulk materials in which the characteristic lengths may be nanometers or micrometers rather than angstroms or atoms. This is an area in which theoretical studies should be particularly useful in interpreting experimental observations and for screening classifications of materials for compatibility to guide future experimentation.

Another challenge is to identify precursors, conditions, and methods (e.g., masking or templating) that could favor deposition onto highly coordinated facets rather than low coordination defects and edge sites. As of now, the demonstrated ALD systems always show preference for initial deposition at low coordination sites. In cases that these low coordination sites are responsible for the chemistry of interest (e.g., many Au-based catalysts), this is an obvious obstacle to employing ALD overcoating. In addition, there are cases that the overcoat could have negative secondary consequences, as was the case with the AlO_x films deposited on Cu catalysts that led to increased blocking of the nanoparticles by coking reactions.[138] In such cases, creative solutions and alternatives to mitigate such unintended consequences need to be explored, as was done with the addition of MgO_x to decrease acidity and coking.[13]

Enhancement of nanoparticle stability is a critically important and already established practical application of ALD, especially for biomass conversion in the liquid-phase. This is an application (the production of "green chemicals") that may justify what is currently an increased cost of making an ALD catalyst. Althugh stabilization of metal nanoparticles is a significant advancement, many opportunities to expand the impact of ALD overcoating still exist. Whereas ALD of oxides, metals, and bimetallics, offers the ability to finely control the distribution of active sites, overcoating with ALD enables the ability to structure microenvironments around an active site and create catalytic architectures. This approach includes the potential to finely tune the spatial distribution of the two active sites to optimize activity and selectivity or modify the composition of the overcoat to alter the hydrophobicity inside the pore (Figure 11). In addition, one can envision tuning the acidity of an overcoat layer by atomically controlling the composition to maximize the desired reactions without catalyzing the formation of less favorable and unwanted side products. In addition to these practical applications, ALD overcoating provides another important tool for the experimentalist to help elucidate reaction mechanisms by selectively blocking active sites.

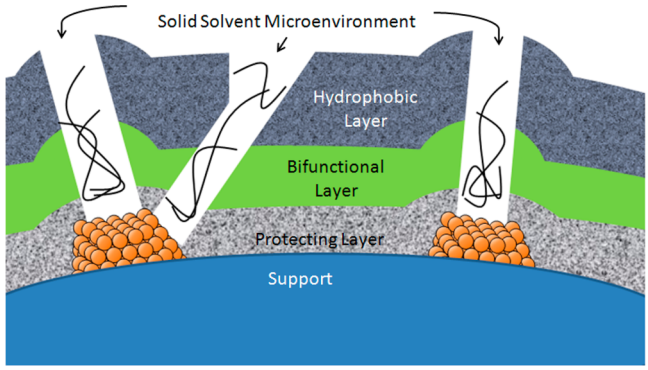

Figure 11. An example of the potential for a tailored active site surrounded by a microenvironment that could be created with the combination ALD/MLD and polymer overcoating. Figure reproduced with permission from Schwartz et al. Copyright 2014, American Chemical Society.[2]

6. OUTLOOK FOR ATOMICALLY DESIGNED ALD CATALYSTS

ALD is a technique for synthesizing catalysts at the atomic level that has gained attention for its application to heterogeneous catalysts in the past few years. ALD provides the ability to synthesize model supported catalysts that can be used to elucidate fundamental catalytic phenomena and offers a number of uniquely powerful opportunities. For example, ALD can "homogenize" supported heterogeneous catalysts by creating nanoparticles with extremely narrow distributions in size and composition, which is essential for understanding the fundamental nature of the catalytic active site. This type of control over the distribution of active sites is critical for elucidating reaction mechanisms that form the foundation for the rational design of improved catalysts. Finally, ALD closes the loop in this catalyst design approach by being an ideal method for synthesizing a rationally designed material with atomic-level precision (Figure 12).

Although the potential to use ALD as a tool for developing fundamental knowledge and facilitating rational design is clear, the continued development of practical applications for ALD catalysts will be essential in motivating sustained interest in the technology. Processes for synthesizing ALD catalysts are oftentimes considered slow and expensive, but this is not inherent to the chemical kinetics of the ALD process, but rather due to limitations of current ALD strategies, equipment, and precursor availability/cost. The microelectronics industry uses ALD on a commercial scale to manufacture a range of different devices. Thus, as the application of ALD in the microelectronics industry matures with the limits of device miniaturization approaching, a broadening of ALD applications within catalysis will become necessary to motivate continued development. Initially, applications in whihc the cost structure is similar to the

DOI: 10.1021/cs501862h
ACS Catal. 2015, 5, 1804−1825

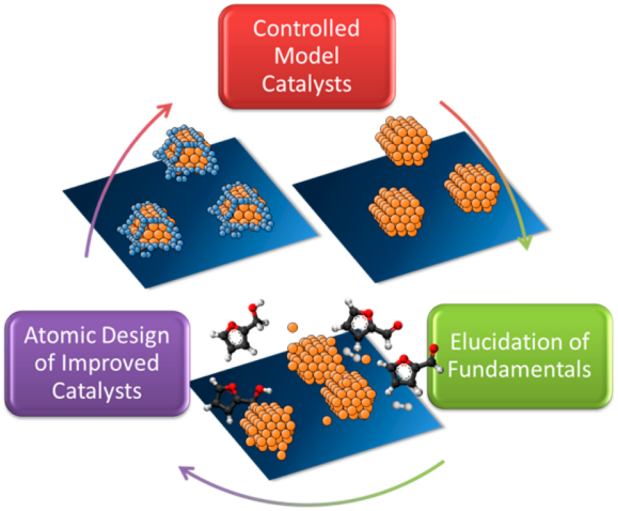

Figure 12. ALD can be used in a feedback loop in order to rationally design catalytic materials. First, model catalysts with controlled distributions of active sites can be synthesized and subsequently used to more clearly elucidate the reaction mechanisms, catalytic fundamentals, and structure−property relationships. After elucidating the fundamentals, the atomic-level control provided by ALD is the ideal way to synthesize ideally designed catalytic architectures.

microelectronics industry (i.e., the final products have very high value in order to justify the investment in ALD) are of primary interest. For example, the creation of highly dispersed and stabilized nanoparticles has intriguing potential because of the high costs associated with precious metal raw materials, process shutdowns for regeneration, catalyst replacement, and disposal. Furthermore, the development of stabilized nanoparticles may be an important hedge against potential environmental damage from leached metals or against future environmental regulations that could significantly increase costs for disposing of metals. The extended lifetime of metal nanoparticle catalysts is one application in which the increased cost of ALD catalysts may be justified, especially in situations that a precious-metal catalyst can be replaced by a base-metal catalyst as a result of the enhanced stability imparted by ALD. Furthermore, applying ALD for stabilization has been demonstrated with only a few cycles of relatively inexpensive precursors, lowering the barrier for adoption. Meanwhile, the ability to build complex catalyst architectures (bifunctionality, spatial control of active sites, tuning of hydrophobicity/hydrophilicity, tuning of acid/base properties) that could tailor the microenvironment around an active site extends ALD catalysts to be potentially applicable to any chemistry and offers possibilities for catalyst customization. This high degree of control and specialization may be another entry way for ALD catalysts because they can be useful for specialized synthesis of high-value-added products (e.g., pharmaceuticals). If ALD catalysts can gain initial adoption through these high-value entries to the catalyst market (stabilization and specialization), it would facilitate the development of scaled-up synthesis processes such as large-scale batch coating, fluidized beds, or continuous spatial ALD.

Development of ALD methods and improvements in reactor design over the last two decades, much of it centered around the development of thin films for electronic materials, have laid the fundamental foundation for ALD of catalytic materials. In just a few years, the atomic precision of ALD has demonstrated important practical and fundamental successes. It has shown potential to address practical catalytic issues, such as creating highly dispersed nanoparticles on high-surface-area supports, finely controlling the composition and morphology of bimetallic nanoparaticles, the imparting of size selectivity, stabilizing metal nanoparticles through the creation of nanobowls and overcoats, and the creation of local microenvironments through the atomic tuning of the properties of overcoat layers. Although it is unknown if ALD synthesis techniques will ever prove commercially viable, the demonstrated potential impacts outlined by the above examples warrant continued examination of ALD process improvements (to drive down costs) as well as investigation of expanded applications (to broaden demand). Furthermore, as discussed throughout this Review, ALD has been used in elucidating mechanisms of catalyst performance such as photonic effects, particle size effects, support effects, and interfacial active sites, which makes it an academically interesting tool for the elucidation of fundamental catalytic science, even if it never finds direct commercial application.

AUTHOR INFORMATION

Corresponding Author

*E-mail: huber@engr.wisc.edu.

Present Address

¶(B.J.O.) ExxonMobil Research and Engineering, Annandale, New Jersey 08833, United States

Notes

The authors declare no competing financial interest.

ACKNOWLEDGMENTS

This material is based upon work supported as part of the Institute for Atom-efficient Chemical Transformations (IACT), an Energy Frontier Research Center funded by the U.S. Department of Energy, Office of Science, Office of Basic Energy Sciences. The authors thank David M. King for useful discussions pertaining to ALD reactor systems.

REFERENCES

(1) Bartholomew, C. H.; Farrauto, R. J. *Fundamentals of Industrial Catalytic Processes*, 2nd ed.,; John Wiley and Sons: New York, 2011, pp 4−12.

(2) Schwartz, T. J.; O'Neill, B. J.; Shanks, B. H.; Dumesic, J. A. *ACS Catal.* **2014**, *4*, 2060−2069.

(3) Adams, C. *Top. Catal.* **2009**, *52*, 924−934.

(4) Lu, J.; Liu, B.; Greeley, J. P.; Feng, Z.; Libera, J. A.; Lei, Y.; Bedzyk, M. J.; Stair, P. C.; Elam, J. W. *Chem. Mater.* **2012**, *24*, 2047−2055.

(5) Enterkin, J. A.; Setthapun, W.; Elam, J. W.; Christensen, S. T.; Rabuffetti, F. A.; Marks, L. D.; Stair, P. C.; Poeppelmeier, K. R.; Marshall, C. L. *ACS Catal.* **2011**, *1*, 629−635.

(6) Christensen, S. T.; Feng, H.; Libera, J. L.; Guo, N.; Miller, J. T.; Stair, P. C.; Elam, J. W. *Nano Lett.* **2010**, *10*, 3047−3051.

(7) Johansson, A. C.; Larsen, J. V.; Verheijen, M. A.; Haugshoj, K. B.; Clausen, H. F.; Kessels, W. M. M.; Christensen, L. H.; Thomsen, E. V. *J. Catal.* **2014**, *311*, 481−486.

(8) Lu, J.; Low, K.-B.; Lei, Y.; Libera, J. A.; Nicholls, A.; Stair, P. C.; Elam, J. W. *Nat. Commun.* **2014**, *5*, 4264.

(9) Lei, Y.; Liu, B.; Lu, J.; Lobo-Lapidus, R. J.; Wu, T.; Feng, H.; Xia, X.; Mane, A. U.; Libera, J. A.; Greeley, J. P.; Miller, J. T.; J. T. Elam, J. T. *Chem. Mater.* **2012**, *24*, 3525−3533.

(10) Lu, J.; Fu, B.; Kung, M. C.; Xiao, G.; Elam, J. W.; Kung, H. H.; Stair, P. C. *Science* **2012**, *335*, 1205−1208.

(11) O'Neill, B. J.; Jackson, D. H. K.; Crisci, A. J.; Farberow, C. A.; Shi, F.; Alba-Rubio, A. C.; Lu, J.; Dietrich, P. J.; Gu, X.; Marshall, C. L.;

DOI: 10.1021/cs501862h
ACS Catal. 2015, 5, 1804−1825

Stair, P. C.; Elam, J. W.; Miller, J. T.; Ribeiro, F. H.; Voyles, P. M.; Greeley, J.; Mavrikakis, M.; Scott, S. L.; Kuech, T. F.; Dumesic, J. A. *Angew. Chem., Int. Ed.* **2013**, *52*, 13808−13812.
(12) Alba-Rubio, A. C.; O'Neill, B. J.; Shi, F.; Akatay, C.; Canlas, C.; Li, T.; Winans, R.; Elam, J. W.; Stach, E. A.; Voyles, P. M.; Dumesic, J. A. *ACS Catal.* **2014**, *4*, 1554−1557.
(13) O'Neill, B. J.; Sener, C.; Jackson, D. H. K.; Kuech, T. F.; Dumesic, J. A. *ChemSusChem* **2014**, *7*, 3247−3251.
(14) Liang, X.; Li, J.; Yu, M.; McMurray, C. N.; Falconer, J. L.; Weimer, A. W. *ACS Catal.* **2011**, *1*, 1162−1165.
(15) Shang, Z. Y.; Patel, R. L.; Evanko, B. W.; Liang, X. H. *Chem. Commun.* **2013**, *49*, 10067−10069.
(16) Lee, J.; Jackson, D. H. K.; Li, T.; Winans, R. E.; Dumesic, J. A.; Kuech, T. F.; Huber, G. W. *Energy Environ. Sci.* **2014**, *7*, 1657−1660.
(17) Gould, T.; Izar, A.; Weimer, A. W.; Falconer, J. L.; Medlin, J. W. *ACS Catal.* **2014**, *4*, 2714−2717.
(18) Parsons, G. N.; Elam, J. W.; George, S. M.; Haukka, S.; Jeon, H.; Kessels, W. M. M.; Leskelä, M.; Poodt, P.; Ritala, M.; Rossnagel, S. M. *J. Vac. Sci. Technol., A* **2013**, *31*, 050818.
(19) Suntola, T.; Antson, J. U.S. Patent US4058430 A, 1977.
(20) Aleskovsky, V.; Koltcov, M. USSR Patent USSR422446, 1972.
(21) Miikkulainen, V.; Leskelä, M.; Ritala, M.; Puurunen, R. L. *J. Appl. Phys.* **2013**, *113*, 021201.
(22) (a) Liang, X. H.; Jiang, C. J. *J. Nanopart. Res.* **2013**, *15*, 1890. (b) Jiang, C. J.; Liang, X. H. *Catal. Commun.* **2014**, *46*, 41−45. (c) Sairanen, E.; Karinen, R.; Borghei, M.; Kauppinen, E. I.; Lehtonen, J. *ChemCatChem.* **2012**, *4*, 2055−2061. (d) Deng, S.; Kurttepeli, M.; Deheryan, S.; Cott, D. J.; Vereecken, P. M.; Martens, J. A.; Bals, S.; van Tendeloob, G.; Detavernier, C. *Nanoscale* **2014**, *6*, 6939−6944. (e) Guder, F.; Frei, E.; Kucukbayrak, U. M.; Menzel, A.; Thomann, R.; Luptak, R.; Holaender, B.; Krossing, I.; Zacharias, M. *ACS Appl. Mater. Interfaces* **2014**, *6*, 1576−1582.
(23) Hsueh, Y. C.; Wang, C. C.; Kei, C. C.; Lin, Y. H.; Liu, C.; Perng, T. P. *J. Catal.* **2012**, *294*, 63−68.
(24) (a) Assaud, L.; Monyoncho, E.; Pitzschel, K.; Allagui, A.; Petit, M.; Hanbucken, M.; Baranova, E. A.; Santinacci, L. *Beilstein J. Nanotechnol.* **2014**, *5*, 162−172. (b) Phillips, R.; Hansen, P.; Eisenbraun, E. *J. Vac. Sci. Technol., A* **2012**, *30*, 6. (c) Xiong, G.; Elam, J. W.; Feng, H.; Han, C. Y.; Wang, H. H.; Iton, L. E.; Curtiss, L. A.; Pellin, M. J.; Kung, M.; Kung, H.; Stair, P. C. *J. Phys. Chem. B* **2005**, *109*, 14059−14063.
(25) Feng, H.; Elam, J. W.; Libera, J. A.; Pellin, M. J.; Stair, P. C. *J. Catal.* **2010**, *269*, 421−431.
(26) (a) Dillon, A. C.; Ott, A. W.; Way, J. D.; George, S. M. *Surf. Sci.* **1995**, *322*, 230−242. (b) Higashi, G. S.; Fleming, C. G. *Appl. Phys. Lett.* **1989**, *55*, 1963−1965.
(27) Aarik, J.; Aidla, A.; Kiisler, A. A.; Uustare, T.; Sammelselg, V. *Thin Solid Films* **1999**, *340*, 110−116.
(28) Ritala, M.; Leskela, M.; Nykanen, E.; Soininen, P.; Niinisto, L. *Thin Solid Films* **1993**, *225*, 288−295.
(29) Hämäläinen, J.; Ritala, M.; Leskelä, M. *Chem. Mater.* **2013**, *26*, 786−801.
(30) Seghete, D.; Rayner, G. B.; Cavanagh, A. S.; Anderson, V. R.; George, S. M. *Chem. Mater.* **2011**, *23*, 1668−1678.
(31) Serp, P.; Kalck, P.; Feurer, R. *Chem. Rev.* **2002**, *102*, 3085−3128.
(32) George, S. M. *Chem. Rev.* **2010**, *110*, 111−131.
(33) Puurunen, R. L. *J. Appl. Phys.* **2005**, *97*, 121301−121352.
(34) Xinye, L.; Ramanathan, S.; Longdergan, A.; Srivastava, A.; Lee, E.; Seidel, T. E.; Barton, J. T.; Dawen, P.; Gordon, R. G. *J. Electrochem. Soc.* **2005**, *152*, 213−219.
(35) Jung, Y. S.; Cavanagh, A. S.; Dillon, A. C.; Groner, M. D.; George, S. M.; Lee, S. H. *J. Electrochem. Soc.* **2010**, *157*, A75−81.
(36) Jackson, D. H. K.; Dunn, B. A.; Guan, Y.; Kuech, T. F. *AIChE J.* **2014**, *60*, 1278−1286.
(37) Elam, J. W.; Schuisky, M.; Ferguson, J. D.; George, S. M. *Thin Solid Films* **2003**, *436*, 145−156.
(38) Rai, V. R.; Agarwal, S. *Chem. Mater.* **2011**, *23*, 2312−2316.
(39) Lu, J. L.; Stair, P. C. *Angew. Chem., Int. Ed.* **2010**, *49*, 2547−2551.
(40) Putkonen, M.; Nieminen, M.; Niinisto, L. *Thin Solid Films* **2004**, *466*, 103−107.
(41) (a) Ferguson, J. D.; Smith, E. R.; Weimer, A. W.; George, S. M. *J. Electrochem. Soc.* **2004**, *151*, 528−535. (b) Jackson, D. H. K.; Wang, D.; Gallo, J. M. R.; Crisci, A. J.; Scott, S. L.; Dumesic, J. A.; Kuech, T. F. *Chem. Mater.* **2013**, *25*, 3844−3851. (c) Klaus, J. W.; Sneh, O.; Ott, A. W.; George, S. M. *Surf. Rev. Lett.* **1999**, *6*, 435−448. (d) Klaus, J. W.; Sneh, O.; George, S. M. *Science* **1997**, *278*, 1934−1936. (e) Du, Y.; Du, X.; George, S. M. *J. Phys. Chem. C* **2007**, *111*, 219−226. (f) Du, Y.; Du, X.; George, S. M. *Thin Solid Films* **2005**, *491*, 43−53.
(42) Klaus, J. W.; George, S. M. *Surf. Sci.* **2000**, *447*, 81−90.
(43) (a) Burton, B. B.; Boleslawski, M. P.; Desombre, A. T.; George, S. M. *Chem. Mater.* **2008**, *20*, 7031−7043. (b) Liang, X.; Barrett, K. S.; Jiang, Y.-B.; Weimer, A. W. *ACS Appl. Mater. Interfaces* **2010**, *2*, 2248−2253.
(44) Profijt, H. B.; Potts, S. E.; van de Sanden, M. C. M.; Kessels, W. M. M. *J. Vac. Sci. Technol., A* **2011**, *29*, 050801.
(45) (a) Van Bui, H.; Kovalgin, A. Y.; Aarnink, A. A. I.; Wolters, R. A. M. *ECS J. Solid State Sci. Technol.* **2013**, *2*, 149−155. (b) Shimizu, H.; Sakoda, K.; Momose, T.; Koshi, M.; Shimogaki, Y. *J. Vac. Sci. Technol., A* **2012**, *30*, 01A144. (c) Yuan, G. J.; Shimizu, H.; Momose, T.; Shimogaki, Y. *J. Vac. Sci. Technol., A* **2014**, *32*, 01A104. (d) Yuan, G.; Shimizu, H.; Momose, T.; Shimogaki, Y. *Microelectron. Eng.* **2014**, *120*, 230−234.
(46) Kim, J. B.; Kwon, D. R.; Chakrabarti, K.; Lee, C.; Oh, K. Y.; Lee, J. H. *J. Appl. Phys.* **2002**, *92*, 6739−6742.
(47) (a) Niinisto, L.; Ritala, M.; Leskela, M. *J. Mater. Sci. Eng. B* **1996**, *41*, 23−29. (b) Kim, S. K.; Hwang, C. S.; Park, S. H. K.; Yun, S. J. *Thin Solid Films* **2005**, *478*, 103−108.
(48) Goldstein, D. N.; McCormick, J. A.; George, S. M. *J. Phys. Chem. C* **2008**, *112*, 19530−19539.
(49) Potts, S. E.; Kessels, W. M. M. *Coord. Chem. Rev.* **2013**, *257*, 3254−3270.
(50) Longrie, D.; Deduytsche, D.; Haemers, J.; Driesen, K.; Detavernier, C. *Surf. Coat. Technol.* **2012**, *213*, 183−191.
(51) Longrie, D.; Deduytsche, D.; Haemers, J.; Smet, P. F.; Driesen, K.; Detavernier, C. *ACS Appl. Mater. Interfaces* **2014**, *6*, 7316−7324.
(52) Liu, X. Y.; Gu, Y. Q.; Huang, J. G. *Chem.—Eur. J.* **2010**, *16*, 7730−7740.
(53) Gong, B.; Kim, D. H.; Parsons, G. N. *Langmuir* **2012**, *28*, 11906−11913.
(54) (a) Detavernier, C.; Dendooven, J.; Sree, S. P.; Ludwig, K. F.; Martens, J. A. *Chem. Soc. Rev.* **2011**, *40*, 5242−5253. (b) Sree, S. P.; Dendooven, J.; Jammaer, J.; Masschaele, K.; Deduytsche, D.; D'Haen, J.; Kirschhock, C. E. A.; Martens, J. A.; Detavernier, C. *Chem. Mater.* **2012**, *24*, 2775−2780. (c) Elam, J. W.; Libera, J. A.; Huynh, T. H.; Feng, H.; Pellin, M. J. *J. Phys. Chem. C* **2010**, *114*, 17286−17292.
(55) Pagán-Torres, Y. J.; Gallo, J. M. R.; Wang, D.; Pham, H. N.; Libera, J. A.; Marshall, C. L.; Elam, J. W.; Datye, A. K.; Dumesic, J. A. *ACS Catal.* **2011**, *1*, 1234−1245.
(56) (a) Vuori, H.; Silvennoinen, R. J.; Lindblad, M.; Osterholm, H.; Krause, A. O. I. *Catal. Lett.* **2009**, *131*, 7−15. (b) Verheyen, E.; Sree, S. P.; Thomas, K.; Dendooven, J.; De Prins, M.; Vanbutsele, G.; Breynaert, E.; Gilson, J. P.; Kirschhock, C. E. A.; Detavernier, C.; Martens, J. A. *Chem. Commun.* **2014**, *50*, 4610−4612. (c) Sree, S. P.; Dendooven, J.; Koranyi, T. I.; Vanbutsele, G.; Houthoofd, K.; Deduytsche, D.; Detavernier, C.; Martens, J. A. *Catal. Sci. Technol.* **2011**, *1*, 218−221.
(57) Vandegehuchte, B. D.; Thybaut, J. W.; Detavernier, C.; Deduytsche, D.; Dendooven, J.; Martens, J. A.; Sree, S. P.; Koranyi, T. I.; Marin, G. B. *J. Catal.* **2014**, *311*, 433−446.
(58) (a) Mackus, A. J. M.; Thissen, N. F. W.; Mulders, J. J. L.; Trompenaars, P. H. F.; Verheijen, M. A.; Bol, A. A.; Kessels, W. M. M. *J. Phys. Chem. C* **2013**, *117*, 10788−10798. (b) Selvaraj, S. K.; Parulekar, J.; Takoudis, C. G. *J. Vac. Sci. Technol., A* **2014**, *32*, 010601. (c) Park, K. J.; Doub, J. M.; Gougousi, T.; Parsons, G. N. *Appl. Phys. Lett.* **2005**, *86*, 051903. (d) Sinha, A.; Hess, D. W.; Henderson, C. L. *J. Vac. Sci. Technol., B* **2007**, *25*, 1721−1728. (e) Sinha, A.; Hess, D. W.; Henderson, C. L. *J. Vac. Sci. Technol., B* **2006**, *24*, 2523−2532.

DOI: 10.1021/cs501862h
ACS Catal. 2015, 5, 1804−1825

(59) Yan, M.; Koide, Y.; Babcock, J. R.; Markworth, P. R.; Belot, J. A.; Marks, T. J.; Chang, R. P. H. *Appl. Phys. Lett.* **2001**, *79*, 1709−1711.
(60) (a) Dasgupta, N. P.; Liu, C.; Andrews, S.; Prinz, F. B.; Yang, P. D. *J. Am. Chem. Soc.* **2013**, *135*, 12932−12935. (b) Gong, B.; Peng, Q.; Na, J. S.; Parsons, G. N. *Appl. Catal., A* **2011**, *407*, 211−216.
(61) Kim, E.; Vaynzof, Y.; Sepe, A.; Guldin, S.; Scherer, M.; Cunha, P.; Roth, S. V.; Steiner, U. *Adv. Funct. Mater.* **2014**, *24*, 863−872.
(62) (a) Gong, B.; Peng, Q.; Parsons, G. N. *J. Phys. Chem. B* **2011**, *115*, 11028−11028. (b) Liang, X. H.; Yu, M.; Li, J. H.; Jiang, Y. B.; Weimer, A. W. *Chem. Commun.* **2009**, 7140−7142.
(63) (a) Rahtu, A.; Ritala, M.; Leskela, M. *Chem. Mater.* **2001**, *13*, 1528−1532. (b) Brahim, C.; Chauveau, F.; Ringuede, A.; Cassir, M.; Putkonen, M.; Niinistoe, L. *J. Mater. Chem.* **2009**, *19*, 760−766. (c) Kasikov, A.; Aarik, J.; Mandar, H.; Moppel, M.; Pars, M.; Uustare, T. *J. Phys. D Appl. Phys.* **2006**, *39*, 54−60.
(64) (a) Elers, K. E.; Saanila, V.; Li, W. M.; Soininen, P. J.; Kostamo, J. T.; Haukka, S.; Juhanoja, J.; Besling, W. F. A. *Thin Solid Films* **2003**, *434*, 94−99. (b) Elam, J. W.; Sechrist, Z. A.; George, S. M. *Thin Solid Films* **2002**, *414*, 43−55. (c) Kaariainen, M. L. Kaariainen, T.; Cameron, D. C. In *SVC 50th Annual Technical Conference Proceedings*; Society of Vacuum Coaters, 2007, 335−339. (d) Zhong, L. J.; Daniel, W. L.; Zhang, Z. H.; Campbell, S. A.; Gladfelter, W. L. *Chem. Vap. Deposition* **2006**, *12*, 143−150.
(65) Rikkinen, E.; Santasalo-Aarnio, A.; Airaksinen, S.; Borghei, M.; Viitanen, V.; Sainio, J.; Kauppinen, E. I.; Kallio, T.; Krause, A. O. I. *J. Phys. Chem. C* **2011**, *115*, 23067−23073.
(66) Masango, S. S.; Peng, L.; Marks, L. D.; Van Duyne, R. P.; Stair, P. C. *J. Phys. Chem. C* **2014**, *118*, 17655−17661.
(67) Feng, H.; Elam, J. W.; Libera, J. A.; Setthapun, W.; Stair, P. C. *Chem. Mater.* **2010**, *22*, 3133−3142.
(68) Nie, A.; Liu, J.; Li, Q.; Cheng, Y.; Dong, C.; Zhou, W.; Wang, P.; Wang, Q.; Yang, Y.; Zhu, Y.; Zeng, Y.; Wang, H. *J. Mater. Chem.* **2012**, *22*, 10665−10671.
(69) Weber, M. J.; Mackus, A. J. M.; Verheijen, M. A.; van der Marel, C.; Kessels, W. M. M. *Chem. Mater.* **2012**, *24*, 2973−2977.
(70) Wank, J. R.; George, S. M.; Weimer, A. W. *Powder Technol.* **2004**, *142*, 59−69.
(71) Tiznado, H.; Zaera, F. *J. Phys. Chem. B* **2006**, *110*, 13491−13498.
(72) (a) Reijnen, L.; Meester, B.; Goossens, A.; Schoonman, J. *Chem. Vap. Deposition* **2003**, *9*, 15−20. (b) Scharf, T. W.; Prasad, S. V.; Mayer, T. M.; Goeke, R. S.; Dugger, M. T. *J. Mater. Res.* **2004**, *19*, 3443−3446. (c) Sinsermsuksakul, P.; Heo, J.; Noh, W.; Hock, A. S.; Gordon, R. G. *Adv. Energy Mater.* **2011**, *1*, 1116−1125.
(73) Nagasawa, H.; Yamaguchi, Y. *Thin Solid Films* **1993**, *225*, 230−234.
(74) Feng, H.; Libera, J. A.; Stair, P. C.; Miller, J. T.; Elam, J. W. *ACS Catal.* **2011**, *1*, 665−673.
(75) (a) Aaltonen, T.; Ritala, M.; Tung, Y. L.; Chi, Y.; Arstila, K.; Meinander, K.; Leskela, M. *J. Mater. Res.* **2004**, *19*, 3353−3358. (b) Kim, S. K.; Han, J. H.; Kim, G. H.; Hwang, C. S. *Chem. Mater.* **2010**, *22*, 2850−2856. Li, J. H.; Liang, X. H.; King, D. M.; Jiang, Y. B.; Weimer, A. W. *Appl. Catal., B* **2010**, *97*, 220−226. Elliott, S. D. *Langmuir* **2010**, *26*, 9179−9182.
(76) Ritala, M.; Leskela, M.; Rauhala, E.; Haussalo, P. *J. Electrochem. Soc.* **1995**, *142*, 2731−2737.
(77) (a) Puurunen, R. L.; Root, A.; Sarv, P.; Haukka, S.; Iiskola, E. I.; Lindblad, M.; Krause, A. O. I. *Appl. Surf. Sci.* **2000**, *165*, 193−202. (b) Liu, H.; Bertolet, D. C.; Rogers, J. W. *Surf. Sci.* **1995**, *340*, 88−100.
(78) Bauer, E. *Z. Kristallogr.* **1958**, *110*, 372−394.
(79) Canlas, C. P.; Lu, J.; Ray, N. A.; Grosso-Giorgano, N. A.; Lee, S.; Elam, J. W.; Winans, R. E.; Van Duyne, R. P.; Stair, P. C.; Notestein, J. M. *Nat. Chem.* **2012**, *4*, 1030−1036.
(80) (a) Parsons, G. N.; Atanasov, S. E.; Dandley, E. C.; Devine, C. K.; Gong, B.; Jur, J. S.; Lee, K.; Oldham, C. J.; Peng, Q.; Spagnola, J. C.; Williams, P. S. *Coord. Chem. Rev.* **2013**, *257*, 3323−3331. (b) Liang, X.; King, D. M.; Groner, M. D.; Blackson, J. H.; Harris, J. D.; George, S. M.; Weimer, A. W. *J. Membr. Sci.* **2008**, *322*, 105−112.
(81) (a) Kayaci, F.; Ozgit-Akgun, C.; Donmez, I.; Biyikli, N.; Uyar, T. *ACS Appl. Mater. Interfaces* **2012**, *4*, 6185−6194. (b) Korhonen, J. T.; Hiekkataipale, P.; Malm, J.; Karppinen, M.; Ikkala, O.; Ras, R. H. A. *ACS Nano* **2011**, *5*, 1967−1974.
(82) George, S. M.; Lee, B. H.; Yoon, B.; Abdulagatov, A. I.; Hall, R. A. *J. Nanosci. Nanotechnol.* **2011**, *11*, 7948−7955.
(83) Sundberg, P.; Karppinen, M. *Beilstein J. Nanotechnol.* **2014**, *5*, 1104−1136.
(84) Dameron, A. A.; Seghete, D.; Burton, B. B.; Davidson, S. D.; Cavanagh, A. S.; Bertrand, J. A.; George, S. M. *Chem. Mater.* **2008**, *20*, 3315−3326.
(85) Abdulagatov, A. I.; Hall, R. A.; Sutherland, J. L.; Lee, B. H.; Cavanagh, A. S.; George, S. M. *Chem. Mater.* **2012**, *24*, 2854−2863.
(86) Longrie, D.; Deduytsche, D.; Detavernier, C. *J. Vac. Sci. Technol., A* **2014**, *32*, 010802.
(87) Libera, J. A.; Elam, J. W.; Pellin, M. J. *Thin Solid Films* **2008**, *516*, 6158−6166.
(88) King, D. M.; Liang, X. H.; Weimer, A. W. *Powder Technol.* **2012**, *221*, 13−25.
(89) Elam, J. W.; Groner, M. D.; George, S. M. *Rev. Sci. Instrum.* **2002**, *73*, 2981−2987.
(90) King, D. M.; Spencer, J. A.; Liang, X.; Hakim, L. F.; Weimer, A. W. *Surf. Coat. Technol.* **2007**, *201*, 9163−9171.
(91) McCormick, J. A.; Cloutier, B. L.; Weimer, A. W.; George, S. M. *J. Vac. Sci. Technol., A* **2007**, *25*, 67−74.
(92) (a) Gordon, R. G.; Hausmann, D.; Kim, E.; Shepard, J. *Chem. Vap. Deposition* **2003**, *9*, 73−78. (b) Yanguas-Gil, A.; Elam, J. W. *Chem. Vap. Deposition* **2012**, *18*, 46−52.
(93) Goulas, A.; van Ommen, J. R. *J. Mater. Chem. A* **2013**, *1*, 4647−4650.
(94) van Ommen, J. R.; Manuel Valverde, J.; Pfeffer, R. *J. Nanopart. Res.* **2012**, *14*, 737.
(95) Hakim, L. F.; Portman, J. L.; Casper, M. D.; Weimer, A. W. *Powder Technol.* **2005**, *160*, 149−160.
(96) King, D. M.; Weimer, A. W.; Lichty, P. U.S. Patent US 20110236575 A1, 2011.
(97) P. T., LLC http://www.pneumaticoat.com/production-ald.html.
(98) Poodt, P.; Cameron, D. C.; Dickey, E.; George, S. M.; Kuznetsov, V.; Parsons, G. N.; Roozeboom, F.; Sundaram, G.; Vermeer, A. *J. Vac. Sci. Technol., A* **2012**, *30*, 010802.
(99) (a) Van Ommen, J. R. U.S. Patent US 20120009343 A1, 2012. (b) van Ommen, J. R.; Kooijman, D.; de Niet, M.; Talebi, M.; Goulas, A. *J. Vac. Sci. Technol., A* **2015**, *33*, 021513.
(100) Ma, Z.; Brown, S.; Howe, J. Y.; Overbury, S. H.; Dai, S. *J. Phys. Chem. C* **2008**, *112*, 9448−9457.
(101) Muylaert, I.; Musschoot, J.; Leus, K.; Dendooven, J.; Detavernier, C.; Van Der Voort, P. *Eur. J. Inorg. Chem.* **2012**, *2012*, 251−260.
(102) Sree, S. P.; Dendooven, J.; Masschaele, K.; Hamed, H. M.; Deng, S.; Bals, S.; Detavernier, C.; Martens, J. A. *Nanoscale* **2013**, *5*, 5001−5008.
(103) Choi, H.; Bae, J. H.; Kim, D. H.; Park, Y. K.; Jeon, J. K. *Materials* **2013**, *6*, 1718−1729.
(104) Haukka, S.; Lakomaa, E. L.; Suntola, T. *Stud. Surf. Sci. Catal.* **1999**, *120*, 715−750.
(105) (a) Suntola, T. *Appl. Surf. Sci.* **1996**, *100*, 391−398. (b) Haukka, S.; Lindblad, M.; Suntola, T. *Appl. Surf. Sci.* **1997**, *112*, 23−29.
(106) Yanguas-Gil, A.; Libera, J. A.; Elam, J. W. *Chem. Mater.* **2013**, *25*, 4849−4860.
(107) (a) Hakuli, A.; Kytokivi, A.; Lakomaa, E. L.; Krause, O. *Anal. Chem.* **1995**, *67*, 1881−1886. (b) Kytökivi, A.; Lindblad, M.; Root, A. *J. Chem. Soc., Faraday Trans.* **1995**, *91*, 941−948.
(108) Lindblad, M.; Lindfors, L. P.; Suntola, T. *Catal. Lett.* **1994**, *27*, 323−336.
(109) (a) Haukka, S.; Suntola, T. *Interface Sci.* **1997**, *5*, 119−128. (b) Kytokivi, A.; Jacobs, J.-P.; Hakuli, A.; Merilainen, J.; Brongersma, H. H. *J. Catal.* **1996**, *162*, 190−197. (c) Lindblad, M.; Haukka, S.; Kytokivi, A.; Lakomaa, E. L.; Rautiainen, A.; Suntola, T. *Appl. Surf. Sci.* **1997**, *121*, 286−291.

DOI: 10.1021/cs501862h
ACS Catal. 2015, 5, 1804−1825

(110) Lu, J. L.; Kosuda, K. M.; Van Duyne, R. P.; Stair, P. C. *J. Phys. Chem. C* **2009**, *113*, 12412−12418.
(111) Keranen, J.; Guimon, C.; Liskola, E.; Auroux, A.; Niinisto, L. *Catal. Today* **2003**, *78*, 149−157.
(112) Muylaert, I.; Musschoot, J.; Leus, K.; Dendooven, J.; Detavernier, C.; Van der Voort, P. *Eur. J. Inorg. Chem.* **2012**, 251−260.
(113) Johnson, A. M.; Quezada, B. R.; Marks, L. D.; Stair, P. C. *Top. Catal.* **2014**, *57*, 177−187.
(114) Gervasini, A.; Carniti, P.; Keränen, J.; Niinistö, L.; Auroux, A. *Catal. Today* **2004**, *96*, 187−194.
(115) Keranen, J.; Auroux, A.; Ek, S.; Niinisto, L. *Appl. Catal., A* **2002**, *228*, 213−225.
(116) Tilley, S. D.; Schreier, M.; Azevedo, J.; Stefik, M.; Graetzel, M. *Adv. Funct. Mater.* **2014**, *24*, 303−311.
(117) Liu, M.; Nam, C.-Y.; Black, C. T.; Kamcev, J.; Zhang, L. *J. Phys. Chem. C* **2013**, *117*, 13396−13402.
(118) Hu, S.; Shaner, M. R.; Beardslee, J. A.; Lichterman, M.; Brunschwig, B. S.; Lewis, N. S. *Science* **2014**, *344*, 1005−1009.
(119) Holladay, J. D.; Hu, J.; King, D. L.; Wang, Y. *Catal. Today* **2009**, *139*, 244−260.
(120) Zandi, O.; Beardslee, J. A.; Hamann, T. W. *J. Phys. Chem. C* **2014**, *118*, 16494−16503.
(121) Lin, Y.; Xu, Y.; Mayer, M. T.; Simpson, Z. I.; McMahon, G.; Zhou, S.; Wang, D. *J. Am. Chem. Soc.* **2012**, *134*, 5508−5511.
(122) Zandi, O.; Hamann, T. W. *J. Phys. Chem. Lett.* **2014**, *5*, 1522−1526.
(123) Rui, L.; Yongjing, L.; Lien-Yang, C.; Sheehan, S. W.; Wangshu, H.; Fan, Z.; Hou, H. J. M.; Dunwei, W. *Angew. Chem., Int. Ed.* **2011**, *50*, 499−502.
(124) Pickrahn, K. L.; Park, S. W.; Gorlin, Y.; Lee, H. B. R.; Jaramillo, T. F.; Bent, S. F. *Adv. Energy Mater.* **2012**, *2*, 1269−1277.
(125) Chen, Y. W.; Prange, J. D.; Duhnen, S.; Park, Y.; Gunji, M.; Chidsey, C. E. D.; McIntyre, P. C. *Nat. Mater.* **2011**, *10*, 539−544.
(126) Scheuermann, A. G.; Prange, J. D.; Gunji, M.; Chidsey, C. E. D.; McIntyre, P. C. *Energy Environ. Sci.* **2013**, *6*, 2487−2496.
(127) Yang, J.; Walczak, K.; Anzenberg, E.; Toma, F. M.; Yuan, G.; Beeman, J.; Schwartzberg, A.; Lin, Y.; Hettick, M.; Javey, A.; Ager, J. W.; Yano, J.; Frei, H.; Sharp, I. D. *J. Am. Chem. Soc.* **2014**, *136*, 6191−6194.
(128) (a) Kungas, R.; Yu, A. S.; Levine, J.; Vohs, J. M.; Gorte, R. J. *J. Electrochem. Soc.* **2013**, *160*, 205−211. (b) Yu, A. S.; Kungas, R.; Vohs, J. M.; Gorte, R. J. *J. Electrochem. Soc.* **2013**, *160*, 1225−1231.
(129) Gong, Y. H.; Palacio, D.; Song, X. Y.; Patel, R. L.; Liang, X. H.; Zhao, X.; Goodenough, J. B.; Huang, K. *Nano Lett.* **2013**, *13*, 4340−4345.
(130) Mubeen, S.; Lee, J.; Singh, N.; Kraemer, S.; Stucky, G. D.; Moskovits, M. *Nat. Nanotechnol.* **2013**, *8*, 247−251.
(131) (a) Scheffe, J. R.; Li, J. H.; Weimer, A. W. *Int. J. Hydrogen Energy* **2010**, *35*, 3333−3340. (b) Scheffe, J. R.; Allendorf, M. D.; Coker, E. N.; Jacobs, B. W.; McDaniel, A. H.; Weimer, A. W. *Chem. Mater.* **2011**, *23*, 2030−2038. (c) Scheffe, J. R.; McDaniel, A. H.; Allendorf, M. D.; Weimer, A. W. *Energy Environ. Sci.* **2013**, *6*, 963−973.
(132) Muhich, C. L.; Evanko, B. W.; Weston, K. C.; Lichty, P.; Liang, X. H.; Martinek, J.; Musgrave, C. B.; Weimer, A. W. *Science* **2013**, *341*, 540−542.
(133) Arifin, D.; Aston, V. J.; Liang, X. H.; McDaniel, A. H.; Weimer, A. W. *Energy Environ. Sci.* **2012**, *5*, 9438−9443.
(134) Zeng, G.; Qiu, J.; Li, Z.; Pavaskar, P.; Cronin, S. B. *ACS Catal.* **2014**, *4*, 3512−3516.
(135) Liu, C.; Wang, C.-C.; Kei, C.-C.; Hsueh, Y.-C.; Perng, T.-P. *Small* **2009**, *5*, 1535−1538.
(136) Enterkin, J. A.; Poeppelmeier, K. R.; Marks, L. D. *Nano Lett.* **2011**, *11*, 993−997.
(137) (a) Wang, H.; Lu, J.; Marshall, C. L.; Elam, J. W.; Miller, J. T.; Liu, H.; Enterkin, J. A.; Kennedy, R. M.; Stair, P. C.; Poeppelmeier, K. R.; Marks, L. D. *Catal. Today* **2014**, *237*, 71−79. (b) Tallarida, M.; Das, C.; Schmeisser, D. *Beilstein J. Nanotechnol.* **2014**, *5*, 77−82.
(138) O'Neill, B. J.; Miller, J. T.; Dietrich, P. J.; Sollberger, F. G.; Ribeiro, F. H.; Dumesic, J. A. *ChemCatChem.* **2014**, *6*, 2493−2496.
(139) Geyer, S. M.; Methaapanon, R.; Johnson, R. W.; Kim, W. H.; Van Campen, D. G.; Metha, A.; Bent, S. F. *Rev. Sci. Instrum.* **2014**, *85*, 055116.
(140) Devloo-Casier, K.; Ludwig, K. F.; Detavernier, C.; Dendooven, J. *J. Vac. Sci. Technol., A* **2014**, *32*, 010801.
(141) (a) Rahtu, A.; Ritala, M. *Chem. Vap. Deposition* **2002**, *8*, 21−28. (b) Matero, R.; Rahtu, A.; Ritala, M. *Chem. Mater.* **2001**, *13*, 4506−4511.
(142) Liang, X.; Li, N.-H.; Weimer, A. W. *Microporous Mesoporous Mater.* **2012**, *149*, 106−110.
(143) (a) Feng, H.; Elam, J. W.; Libera, J. A.; Pellin, M. J.; Stair, P. C. *Chem. Eng. Sci.* **2009**, *64*, 560−567. (b) Stair, P. C.; Marshall, C. L.; Xiong, G.; Feng, H.; Pellin, M. J.; Elam, J. W.; Curtiss, L.; Iton, L.; Kung, H.; Kung, M.; Wang, H. H. *Top. Catal.* **2006**, *39*, 181−186. (c) Tyo, E. C.; Yin, C. R.; Di Vece, M.; Qian, Q.; Kwon, G.; Lee, S.; Lee, B.; DeBartolo, J. E.; Seifert, S.; Winans, R. E.; Si, R.; Ricks, B.; Goergen, S.; Rutter, M.; Zugic, B.; Flytzani-Stephanopoulos, M.; Wang, Z. W.; Palmer, R. E.; Neurock, M.; Vajda, S. *ACS Catal.* **2012**, *2*, 2409−2423. (d) Biener, M. M.; Biener, J.; Wichmann, A.; Wittstock, A.; Baumann, T. F.; Baumer, M.; Hamza, A. V. *Nano Lett.* **2011**, *11*, 3085−3090. (e) Wittstock, A.; Wichmann, A.; Baeumert, M. *ACS Catal.* **2012**, *2*, 2199−2215. (f) Wichmann, A.; Wittstock, A.; Frank, K.; Biener, M. M.; Neumann, B.; Madler, L.; Biener, J.; Rosenauer, A.; Baumer, M. *ChemCatChem.* **2013**, *5*, 2037−2043.
(144) Lobo, R.; Marshall, C. L.; Dietrich, P. J.; Ribeiro, F. H.; Akatay, C.; Stach, E. A.; Mane, A.; Lei, Y.; Elam, J.; Miller, J. T. *ACS Catal.* **2012**, *2*, 2316−2326.
(145) She, X.; Kwak, J. H.; Sun, J.; Hu, J.; Hu, M. Y.; Wang, C.; Peden, C. H. F.; Wang, Y. *ACS Catal.* **2012**, *2*, 1020−1026.
(146) Suntola, T.; Haukka, S.; Kytökivi, A.; Lakomaa, E. L.; Lindblad, M.; Hietala, J.; Hokkanen, H.; Knuuttila, H.; Knuuttila, P.; Krause, O. U.S. PatentUS6500780 B1, 2002.
(147) (a) Lakomaa, E. L. *Appl. Surf. Sci.* **1994**, *75*, 185−196. (b) Lakomaa, E. L.; Root, A.; Suntola, T. *Appl. Surf. Sci.* **1996**, *107*, 107−115.
(148) Ribeiro, F. H.; Somorjai, G. A. *Recl.: J. R. Neth. Chem. Soc.* **1994**, *113*, 419−422.
(149) Narayanan, S.; Uma, K. *J. Chem. Soc., Faraday Trans. 1* **1985**, *81*, 2733−2744.
(150) Kim, D. H.; Sim, J. K.; Lee, J.; Seo, H. O.; Jeong, M. G.; Kim, Y. D.; Kim, S. H. *Fuel* **2013**, *112*, 111−116.
(151) Elam, J. W.; Zinovev, A.; Han, C. Y.; Wang, H. H.; Welp, U.; Hryn, J. N.; Pellin, M. J. *Thin Solid Films* **2006**, *515*, 1664−1673.
(152) Lee, C.; Yoon, H. K.; Moon, S.; Yoon, K. J. *Korean J. Chem. Eng.* **1998**, *15*, 590−595.
(153) Elam, J. W.; Pellin, M. J.; Stair, P. C. U.S. Patent US7713907 B2, 2010.
(154) Setthapun, W.; Williams, W. D.; Kim, S. M.; Feng, H.; Elam, J. W.; Rabuffetti, F. A.; Poeppelmeier, K. R.; Stair, P. C.; Stach, E. A.; Ribeiro, F. H.; Miller, J. T.; Marshall, C. L. *J. Phys. Chem. C* **2010**, *114*, 9758−9771.
(155) Christensen, S. T.; Elam, J. W.; Rabuffetti, F. A.; Ma, Q.; Weigand, S. J.; Lee, B.; Seifert, S.; Stair, P. C.; Poeppelmeier, K. R.; Hersam, M. C.; Bedzyk, M. J. *Small* **2009**, *5*, 750−757.
(156) King, J. S.; Wittstock, A.; Biener, J.; Kucheyev, S. O.; Wang, Y. M.; Baumann, T. F.; Giri, S. K.; Hamza, A. V.; Baeumer, M.; Bent, S. F. *Nano Lett.* **2008**, *8*, 2405−2409.
(157) Biener, J.; Baumann, T. F.; Wang, Y.; Nelson, E. J.; Kucheyev, S. O.; Hamza, A. V.; Kemell, M.; Ritala, M.; Leskela, M. *Nanotechnology* **2007**, *18*, 055303.
(158) Vuori, H.; Pasanen, A.; Lindblad, M.; Valden, M.; Niemela, M. V.; Krause, A. O. I. *Appl. Surf. Sci.* **2011**, *257*, 4204−4210.
(159) Silvennoinen, R. J.; Jylha, O. J. T.; Lindblad, M.; Osterholm, H.; Krause, A. O. I. *Catal. Lett.* **2007**, *114*, 135−144.
(160) Fu, B. S.; Lu, J. L.; Stair, P. C.; Xiao, G. M.; Kung, M. C.; Kung, H. H. *J. Catal.* **2013**, *297*, 289−295.

DOI: 10.1021/cs501862h
ACS Catal. 2015, 5, 1804−1825

(161) Atesin, A. C.; Ray, N. A.; Stair, P. C.; Marks, T. J. *J. Am. Chem. Soc.* **2012**, *134*, 14682−14685.
(162) Cheng, G.; Wu, Q.; Shang, Z.; Liang, X.; Lin, X. *ChemCatChem.* **2014**, *6*, 2129−2133.
(163) Geus, J. W.; van Dillen, A. J. In *Handbook of Heterogeneous Catalysis*; Ertl, G., Knözinger, H., Schüth, F., Weitkamp, J., Eds.; VCH: Weinheim, 2008, pp 428−467.
(164) (a) Rabuffetti, F. A.; Kim, H.-S.; Enterkin, J. A.; Wang, Y.; Lanier, C. H.; Marks, L. D.; Poeppelmeier, K. R.; Stair, P. C. *Chem. Mater.* **2008**, *20*, 5628−5635. (b) Hu, L.; Wang, C.; Lee, S.; Winans, R. E.; Marks, L. D.; Poeppelmeier, K. R. *Chem. Mater.* **2013**, *25*, 378−384. (c) Lin, Y. Y.; Wen, J. G.; Hu, L. H.; Kennedy, R. M.; Stair, P. C.; Poeppelmeier, K. R.; Marks, L. D. *Phys. Rev. Lett.* **2013**, *111*, 156101.
(165) Winterbottom, W. L. *Acta Metall.* **1967**, *15*, 303−&.
(166) Wulff, G. *Z. Kristallogr.* **1901**, *34*, 449−530.
(167) Enterkin, J. A.; Kennedy, R. M.; Lu, J.; Elam, J. W.; Cook, R. E.; Marks, L. D.; Stair, P. C.; Marshall, C. L.; Poeppelmeier, K. R. *Top. Catal.* **2013**, *56*, 1829−1834.
(168) Mondloch, J. E.; Bury, W.; Fairen-Jimenez, D.; Kwon, S.; DeMarco, E. J.; Weston, M. H.; Sarjeant, A. A.; Nguyen, S. T.; Stair, P. C.; Snurr, R. Q.; Farha, O. K.; Hupp, J. T. *J. Am. Chem. Soc.* **2013**, *135*, 10294−10297.
(169) Baumann, T. F.; Biener, J.; Wang, Y. M.; Kucheyev, S. O.; Nelson, E. J.; Satcher, J. H.; Elam, J. W.; Pellin, M. J.; Hamza, A. V. *Chem. Mater.* **2006**, *18*, 6106−6108.
(170) (a) Chien-Te, H.; Wei-Yu, C.; Dong-Ying, T.; Roy, A. K.; Han-Tsung, H. *Int. J. Hydrogen Energy* **2012**, *37*, 17837−17843. (b) Hsieh, C. T.; Liu, Y. Y.; Tzou, D. Y.; Chen, W. Y. *J. Phys. Chem. C* **2012**, *116*, 26735−26743.
(171) Ferguson, J. D.; Weimer, A. W.; George, S. M. *Thin Solid Films* **2000**, *371*, 95−104.
(172) Wank, J. R.; George, S. M.; Weimer, A. W. *J. Am. Ceram. Soc.* **2004**, *87*, 762−765.
(173) (a) Joo, S. H.; Park, J. Y.; Tsung, C.-K.; Yamada, Y.; Yang, P.; Somorjai, G. A. *Nat. Mater.* **2009**, *8*, 126−131. (b) Yin, Y.; Rioux, R. M.; Erdonmez, C. K.; Hughes, S.; Somorjai, G. A.; Alivisatos, A. P. *Science* **2004**, *304*, 711−714.
(174) Lu, J.; Elam, J. W.; Stair, P. C. *Acc. Chem. Res.* **2013**, *46*, 1806−1815.
(175) Behrens, M.; Studt, F.; Kasatkin, I.; Kühl, S.; Hävecker, M.; Abild-Pedersen, F.; Zander, S.; Girgsdies, F.; Kurr, P.; Kniep, B.-L.; Tovar, M.; Fischer, R. W.; Nørskov, J. K.; Schlögl, R. *Science* **2012**, *336*, 893−897.
(176) Hakim, L. F.; Blackson, J.; George, S. M.; Weimer, A. W. *Chem. Vap. Deposition* **2005**, *11*, 420−425.
(177) Ray, N. A.; Van Duyne, R. P.; Stair, P. C. *J. Phys. Chem. C* **2012**, *116*, 7748−7756.
(178) Feng, H.; Lu, J. L.; Stair, P. C.; Elam, J. W. *Catal. Lett.* **2011**, *141*, 512−517.
(179) Liang, X. H.; Evanko, B. W.; Izar, A.; King, D. M.; Jiang, Y. B.; Weimer, A. W. *Microporous Mesoporous Mater.* **2013**, *168*, 178−182.
(180) Greeley, J. *Electrochim. Acta* **2010**, *55*, 5545−5550.
(181) Zhang, H.; Lei, Y.; Kropf, A. J.; Zhang, G.; Elam, J. W.; Miller, J. T.; Sollberger, F.; Ribeiro, F.; Akatay, M. C.; Stach, E. A.; Dumesic, J. A.; Marshall, C. L. *J. Catal.* **2014**, *317*, 284−292.
(182) (a) Kim, D. W.; Kim, K. D.; Seo, H. O.; Dey, N. K.; Kim, M. J.; Kim, Y. D.; Lim, D. C.; Lee, K. H. *Catal. Lett.* **2011**, *141*, 854−859. (b) Seo, H. O.; Sim, J. K.; Kim, K. D.; Kim, Y. D.; Lim, D. C.; Kim, S. H. *Appl. Catal., A* **2013**, *451*, 43−49.
(183) Zeitsch, K. J. *The chemistry and technology of furfural and its many by-products*; Elsevier: Amsterdam, The Netherlands, 2000; Vol. *13*.
(184) Kumar, M. K.; Krishnamoorthy, S.; Tan, L. K.; Chiam, S. Y.; Tripathy, S.; Gao, H. *ACS Catal.* **2011**, *1*, 300−308.
(185) Shiju, N. R.; Liang, X. H.; Weimer, A. W.; Liang, C. D.; Dai, S.; Guliants, V. V. *J. Am. Chem. Soc.* **2008**, *130*, 5850−5851.

DOI: 10.1021/cs501862h
ACS Catal. 2015, 5, 1804−1825